Civil Engineering and Applied Solutions

Research Article

journal homepage: ceas.journals.umz.ac.ir

CEAS Civil Engineering and Applied Solutions

ANN-Based Modeling of Shear Behavior of Reinforced Concrete Columns under Constant Axial Loads

Maedeh Sadeghpour Haji [a], Reza Niknam [a], Javad Shayanfar [c*]

[a] *Department of Civil Engineering., Islamic Azad University, Qaemshahr, Iran*

[b] *Department of Civil Engineering, University of Minho, Azurém, Guimarães 4800-058, Portugal*

A R T I C L E I N F O

Keywords:
Reinforced concrete columns
Shear behavior
Artificial neural networks (ANN)
Variable axial load
Nonlinear modeling
Seismic performance

Article history:
Received 07 October 2025
Accepted 18 November 2025
Available online 01 February 2026

A B S T R A C T

Many older reinforced concrete (RC) buildings designed under outdated seismic codes exhibit inadequate shear capacity, leading to brittle column failures during earthquakes. Accurate prediction of shear strength is therefore essential for nonlinear seismic assessment. This study develops an analytical–computational framework using artificial neural networks (ANNs) to model the nonlinear flexural–shear behavior of RC columns subjected to constant axial loads. A fiber-based flexural model was formulated, while shear strength was estimated through a Mohr's circle–based approach enhanced with a ductility-dependent degradation parameter. An ANN trained on 164 experimental column tests provided highly accurate shear predictions, outperforming existing analytical models. The framework was validatated against independent experiments confirmed its reliability. The proposed ANN-based approach offers a practical tool for seismic performance evaluation and retrofit design of deficient RC columns.

1. Introduction

The poor performance of many older reinforced concrete (RC) buildings during past earthquakes has highlighted their vulnerability to seismic forces and stresses. These structures were designed and constructed according to codes and standards that do not satisfy the requirements of modern seismic provisions. Post-earthquake field investigations have shown that one of the most critical shortcomings of RC structures designed under older codes is the insufficient shear strength of columns and beams. This weakness often results in brittle shear failure, which subsequently reduces the axial load-carrying capacity of columns and leads to combined shear–axial failures. Documented examples of such damage were observed during the 1971 San Fernando earthquake in the United States [1], the 1994 Northridge earthquake in the United States [1], and the 1999 Kocaeli [2] and Düzce [2] earthquakes in Turkey (Fig. 1). Since the behavior of structures designed according to older codes is generally governed by shear failure in their members, the shear behavior of the structural elements must be carefully considered in the seismic assessment and evaluation of such structures [3-7]. If necessary, the seismic performance of the structure should be enhanced through appropriate shear-strengthening techniques (such as [8-16]) so that it meets the requirements of current seismic design codes.

As has been clearly established, axial load is one of the most important parameters in determining the nonlinear behavior of reinforced concrete columns [3]. It significantly influences the yielding range of the longitudinal reinforcement (moment and curvature at yield), the ductility level of the column, and the ultimate flexural and shear strength of the member. Axial load can affect the behavior of columns in three ways: (a) Compressive axial load can increase the depth of the neutral axis and reduce the flexural cracking zone. (b) The angle of diagonal shear cracks can increase with higher axial load. (c) The width of both shear and flexural cracks can be reduced (enhancing the shear transfer capacity) with an increase in axial load. However, most exiting formulation for shear strength of RC column do not cosider the effect of axial load level. Numerous experimental studies [17-25] have investigated the influence of axial load and reinforcement detailing on the shear performance of RC members. Baldwin and

* Corresponding author.
E-mail addresses: arch3d.ir@gmail.com (J. Shayanfar).

https://doi.org/10.22080/ceas.2025.30228.1050
ISSN: 3092-7749/© 2026 The Author(s). Published by University of Mazandaran.

How to cite this article: Sadeghpour Haji, M., Niknam, R., Shayanfar, J. ANN-Based Modeling of Shear Behavior of Reinforced Concrete Columns under Constant Axial Loads 2026; 2(2): 28–48. doi:10.22080/ceas.2025.30228.1050.

Viest [17] demonstrated the positive contribution of axial load to shear strength, improving diagonal cracking resistance and ultimate shear capacity. Yamad [18] reported that higher axial load ratios and shorter shear spans reduce ductility.

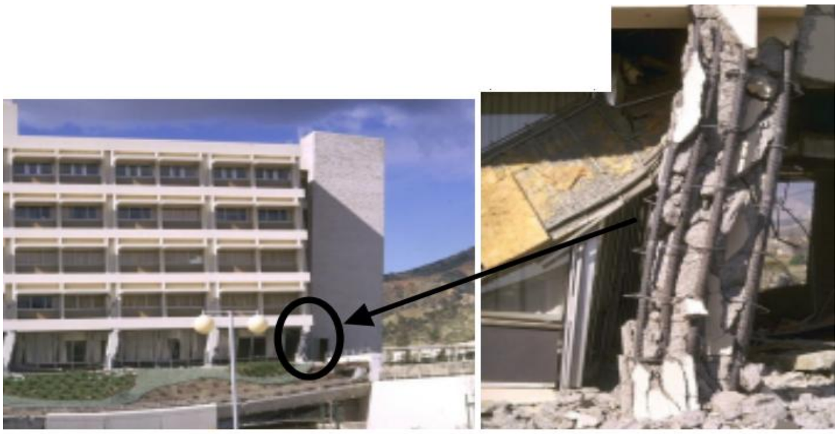

(a) 1971 San Fernando – USA [1].

(b) 1994 Northridge – USA [1].

(c) 1999 Kocaeli – Turkey [2].

(d) 1999 Düzce – Turkey [2].

Fig. 1. Documented damage and failure of reinforced concrete structures observed in past earthquakes.

While Elzanaty et al. [19] showed that higher longitudinal reinforcement ratios enhance shear resistance in beams without stirrups, though less effectively than their contribution to flexural strength. Wight James and Sozen Mete [20], Woodward Kyle and Jirsa James [21], Ascheim and Moehle [22], Ghee et al. [23], Yuk-Lung Wong and Priestley [24] and Bengar et al. [25] further emphasized the dependency of shear strength and ductility on axial load, shear span ratio, and transverse reinforcement. Similarly, Lynn [26], Pan and Li [27], and Duong et al. [28] confirmed the interplay between axial load level, reinforcement configuration, and nonlinear behavior of RC columns.

Experimental studies conducted by [29-33] have demonstrated that the shear strength of concrete members is a function of their flexural deformations. Although current seismic design codes do not explicitly define the reduction of shear capacity as a function of member deformations, the decrease in shear capacity of concrete members under seismic loads is nevertheless considered. For instance, ACI 318 [34] neglects the contribution of concrete to the shear capacity of members subjected to low axial loads. Similarly, FEMA 273 [35] disregards the contribution of concrete to shear strength at moderate and high levels of ductility, and the NZS [36] code does not account for the concrete contribution to shear capacity of members.

In recent years, artificial neural networks (ANNs) have attracted increasing attention due to their capability to evaluate and predict structural behavior by learning from experimental data [37-42]. As accurately estimating the shear capacity of RC members is essential for reliable nonlinear analysis, ANNs provide an effective tool for this purpose. By compiling experimental databases of RC members failing in shear or combined shear–flexure and incorporating key governing parameters as inputs, ANN models can be trained to provide accurate predictions of shear strength. Developing such models forms a key objective of the present research. In this context, the present study aims to develop an advanced modeling framework for predicting the nonlinear shear behavior of reinforced concrete columns designed according to older seismic codes. To achieve this, an extensive experimental database was compiled and used to train artificial neural networks (ANNs), with key geometric, material, and loading parameters as inputs. The ANN-based model was then validated against independent test data and benchmarked against existing analytical models. The results of this study provide a reliable tool for assessing the seismic performance of deficient RC columns and offer valuable insights for strengthening strategies and future code development.

2. Research significance

The shear capacity of RC columns is strongly influenced by ductility demands, which increase under seismic loading and flexural deformations. Conventional analytical formulations often neglect the reduction of shear strength at higher ductility levels, leading to conservative or inaccurate predictions, particularly for RC members designed according to older seismic codes. This study addresses this gap by integrating the effects of ductility on shear capacity within an ANN framework. By leveraging experimental data and key governing parameters, the ANN model provides accurate, data-driven predictions of shear strength, capturing the complex interaction between flexural deformations, axial load, and reinforcement detailing. The proposed approach offers a practical and reliable tool for assessing the nonlinear shear behavior of deficient RC columns, supporting improved seismic evaluation, retrofitting strategies, and informed updates to design codes.

3. ANN-based shear modeling of RC columns under constant axial load

Previous studies have shown that one of the deficiencies of structures designed according to older codes is their vulnerability and lack of shear strength in columns and beams [2]. This deficiency often leads to undesirable shear failure, which, through the reduction of the column's axial capacity, can result in combined shear–axial failure. Such behavior can cause a significant reduction in the member's strength and ductility response. On the other hand, experimental studies [29-33] have demonstrated that the shear strength of concrete members is a function of their flexural deformations. Under seismic loading, as flexural deformations increase beyond the yielding of tensile reinforcement, the widening of flexural cracks, crushing and tensile cracking of concrete in the compression zone, and the reduction in neutral axis depth at large deformations collectively lead to a decrease in the shear capacity of reinforced concrete members. Therefore, accounting for the influence of shear mechanisms as a function of flexural deformations in the nonlinear analysis of reinforced concrete members and structures is essential.

In the present study, an analytical model is proposed to calculate the shear capacity of reinforced concrete columns, based on the works of Park et al. [43] and Shayanfar and Akbarzadeh Bengar [3]. According to Mohr's circle theory, the principal compressive (σc) and tensile (σt) stresses at any element within the cross-section of the reinforced concrete member (as illustrated in Fig. 2) can be expressed as follows:

$$\sigma_c = \frac{\sigma}{2} + \sqrt{\frac{\sigma^2}{4} + \nu^2} \tag{1}$$

$$\sigma_c = \frac{\sigma}{2} - \sqrt{\frac{\sigma^2}{4} + \nu^2} \tag{2}$$

where v and σ represent the shear and normal stresses, respectively, at the considered element of the cross-section. Based on Eqs. 1 and 2, the shear stress capacity can be expressed as follows:

$$\nu_c(y_i) = \sqrt{\overline{\sigma_c}[\overline{\sigma_c} - \sigma(y_i)]} \tag{3}$$

$$\nu_t(y_i) = \sqrt{\overline{\sigma_t}[\overline{\sigma_t} + \sigma(y_i)]} \tag{4}$$

$$\nu_{tot} = \sum \nu(y_i) \times bc = \sum min\left(\sqrt{\overline{\sigma_t}[\overline{\sigma_t} + \overline{\sigma}]}, \sqrt{\overline{\sigma_c}[\overline{\sigma_c} - \overline{\sigma}]}\right) \times bc \tag{5}$$

where yi is the distance of each strip element of the cross-section from the neutral axis c. $\overline{\sigma_c}$ and $\overline{\sigma_t}$ represent the compressive and tensile failure levels, respectively, which are selected based on the Rankine failure criteria (Chen [44]) (see Fig. 2). The shear stress capacity $\nu(y_i)$, accounting for the combined contribution of concrete and transverse reinforcement, is taken as the smaller value between $\nu_c(y_i)$ and $\nu_t(y_i)$. According to the shear models proposed by Priestley et al. [45] and Sezen and Moehle Jack [46], if 80% of the cross-sectional area is considered as the effective shear area, and the axial stress in the compression zone of the section ($\sigma = \sum \sigma(y_i)$) is assumed to be equal to the equivalent longitudinal stress induced by the axial load applied to the column ($\bar{\sigma} = N/A_g$), leading to $\bar{\sigma} = \sigma$, the shear stress capacity can be expressed as follows:

$$\nu_c(y_i) = \sqrt{\overline{\sigma_c}[\overline{\sigma_c} - \sigma]} \tag{6}$$

$$\nu_t(y_i) = \sqrt{\overline{\sigma_t}[\overline{\sigma_t} + \sigma]} \tag{7}$$

Therefore, in all effective shear elements (both tension- and compression-controlled regions), the longitudinal stress, and consequently the shear stress is assumed to be the same. As a result, the member's shear stress capacity ν_c, which is equal to the sum of the shear stresses in all elements within the compression zone of the cross-section $\nu(y_i)$ (taken as the smaller value between $\nu_t(y_i)$ and $\nu_c(y_i)$, can be expressed as:

$$\nu = \sum min[\nu_t(y_i), \nu_c(y_i)] = \sum min\left(\sqrt{\overline{\sigma_t}[\overline{\sigma_t} + \bar{\sigma}]}, \sqrt{\overline{\sigma_c}[\overline{\sigma_c} - \bar{\sigma}]}\right) \tag{8}$$

Since most of the effective shear regions are tension-controlled, it is assumed in this study that member failure is governed by tension-controlled behavior [46]. Therefore:

$$\nu = \sqrt{\overline{\sigma_t}[\overline{\sigma_t} + \bar{\sigma}]} \tag{9}$$

$$\nu_c = \nu \times A_g = \nu \times 0.8\, A_g = 0.8\, A_g \times \sqrt{\overline{\sigma_t}[\overline{\sigma_t} + \bar{\sigma}]} \tag{10}$$

It is worth noting that the principal tensile stress $\overline{\sigma_t}$ represents the combined contribution of concrete and transverse reinforcement to the shear capacity. However, the above relationships do not introduce any parameter to account for the effects of flexural deformation on the shear strength of the concrete member. Therefore, following Sezen and Moehle Jack [46], the parameter λ is defined as a function of displacement ductility (see Fig. 3). In this model, in addition to accounting for the effects of shear deformations on the column's shear capacity, the negative impact of shear deformations on the contribution of transverse reinforcement to the column's shear strength due to reduced anchorage of the transverse barsnis also considered. This parameter can be calculated as follows:

$$\lambda = \begin{cases} 1 & \mu_\Delta \le 2 \\ 1.15 - 0.075\, \mu_\Delta & 2 \le \mu_\Delta \le 6 \\ 0.7 & \mu_\Delta \ge 6 \end{cases} \tag{11}$$

Consequently:

$$\nu = \lambda\sqrt{\overline{\sigma_t}[\overline{\sigma_t} + \bar{\sigma}]} \tag{12}$$

Therefore, using the above relationship, the shear capacity of a reinforced concrete member can be determined as a function of displacement ductility. However, this relationship requires the determination of λ as an input parameter.

Recently, the training of artificial neural networks (ANNs), which are capable of identifying and predicting system mechanisms due to their significant computational intelligence, has attracted considerable attention in the field of civil engineering. For predicting the nonlinear behavior of reinforced concrete members, the development of ANNs can serve as a useful tool, providing both ease of use and high accuracy to meet the requirements of designers and analysts. Therefore, by providing a database of key parameters governing the behavioral mechanisms of reinforced concrete members as input variables, and $\overline{\sigma_t}$ as the output variable, an efficient artificial neural network can be trained. Achieving such a trained network constitutes one of the primary objectives of this paper.

3.1. Experimental database

The output predicted by any ANN is entirely dependent on the samples provided in the database. On the other hand, the nonlinear behavior of reinforced concrete members can be controlled based on their failure mode. In other words, the ultimate strength of a member is a function of the type of failure, such as flexural, flexure–shear, or shear. For columns exhibiting flexure–shear or shear mechanisms, the ultimate strength corresponds to the maximum shear capacity. Therefore, since the focus of this study is on evaluating the performance of structures designed according to older codes (where member failure modes are generally governed by shear mechanisms) the failure modes of the database samples must be either shear or flexure–shear.

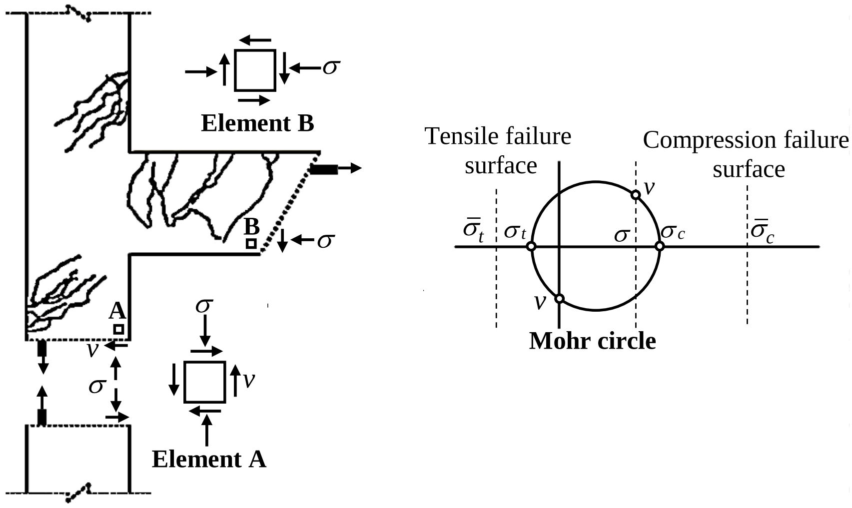

Fig. 2. Rankine failure criteria for concrete in principal stress space (after Chen [44]).

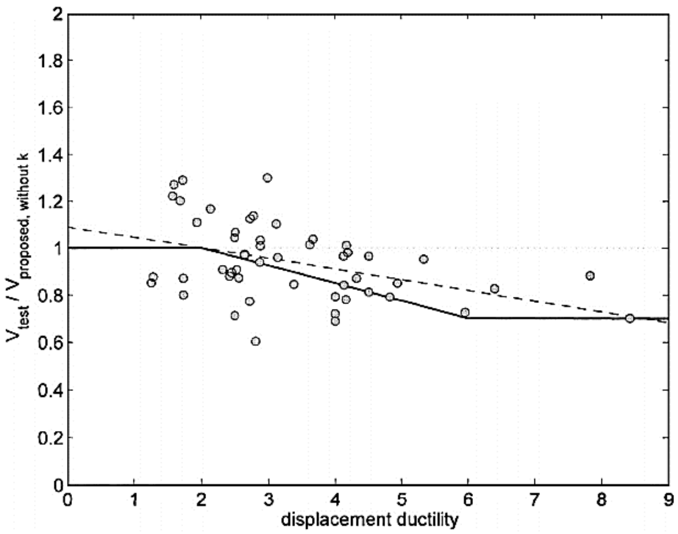

Fig. 3. Degradation parameter as a function of displacement ductility (after Sezen and Moehle Jack [46]).

Consequently, an ANN trained using such a database can identify and predict the flexure–shear or shear mechanisms of the member. In this study, a database of 164 RC column specimens exhibiting shear or flexure–shear failure was compiled from the literature [2, 20, 26, 27, 32, 47-69]. Input parameters included column geometry, longitudinal and transverse reinforcement ratios, axial load ratio, and concrete compressive strength. The database of specimens is summarized in Table 1.

Table 1. Experimental database of RC column specimens with shear or flexure–shear failure modes, including geometric, reinforcement, material, and axial load parameters.

		Input										Other				Output
ID		b (mm)	h (mm)	d (mm)	a (mm)	s (mm)	ρl (%)	fyl (MPa)	ρt (%)	fyt (MPa)	f 'c (MPa)	rN	λ	V (kN)	v (MPa)	$\frac{\sigma_t}{\sqrt{f_c'}}$
Sezen [2]	1	457	457	394	1473	305	2.5	447	0.17	469	21.1	0.15	0.99	314.9	1.90	0.19
	2	457	457	394	1473	305	2.5	447	0.17	469	21.1	0.61	1.00	358.5	2.15	0.08
	3	457	457	394	1473	305	2.5	447	0.17	469	20.9	0.51	1.00	301.1	1.80	0.06
	4	457	457	394	1473	305	2.5	447	0.17	469	21.8	0.15	0.98	294.5	1.80	0.17
Lynn [26]	3CL H18	457	457	381	1473	457	3.1	335	0.07	400	25.6	0.09	1.00	272.1	1.63	0.16
	3SL H18	457	457	381	1473	457	3.1	335	0.07	400	25.6	0.09	1.00	273.1	1.63	0.16
	2CL H18	457	457	381	1473	457	1.9	335	0.07	400	33.1	0.07	0.77	243.2	1.89	0.18
	2SL H18	457	457	381	1473	457	1.9	335	0.07	400	33.1	0.07	0.97	231.0	1.43	0.12
	2CM H18	457	457	381	1473	457	1.9	335	0.07	400	25.7	0.28	1.00	307.8	1.84	0.09
	3CM H18	457	457	381	1473	457	3.1	335	0.07	400	27.6	0.26	1.00	326.9	1.96	0.09
	3CM D12	457	457	381	1473	305	3.1	335	0.17	400	27.6	0.26	1.00	356.0	2.13	0.11
	3SM D12	457	457	381	1473	305	3.1	335	0.17	400	25.7	0.28	1.00	367.2	2.20	0.12

Ohue et al. [47]	2D16RS	200	200	175	400	50	2.0	376	0.57	322	32.1	0.14	0.94	102.0	3.41	0.32
	4D13RS	200	200	175	400	50	2.5	377	0.57	322	29.9	0.15	0.99	111.0	3.49	0.34
Esaki [48]	H-2-1/5	200	200	175	400	50	2.5	363	0.52	370	23.0	0.18	0.85	103.0	3.79	0.47
	HT-2-1/5	200	200	175	400	75	2.5	363	0.52	370	20.2	0.20	0.92	102.0	3.46	0.44
	H-2-1/3	200	200	175	400	40	2.5	363	0.65	370	23.0	0.29	0.97	121.0	3.88	0.37
	HT-2-1/3	200	200	175	400	60	2.5	363	0.65	370	20.2	0.29	0.96	112.0	3.63	0.38
Li [49]	U-7	400	400	375	1000	120	2.4	581	0.47	382	29.0	0.10	0.85	328.0	3.01	0.35
	U-8	400	400	375	1000	120	2.4	581	0.52	382	33.5	0.20	1.00	393.0	3.07	0.21
	U-9	400	400	375	1000	120	2.4	581	0.57	382	34.1	0.30	0.93	430.0	3.62	0.20
Saatcioglu and Ozcebe [50]	U1	350	350	305	1000	150	3.3	430	0.30	470	43.6	0.00	0.95	274.9	2.95	0.45
	U2	350	350	305	1000	150	3.3	453	0.30	470	30.2	0.16	1.00	270.0	2.76	0.23
	U3	350	350	305	1000	75	3.3	430	0.60	470	34.8	0.14	1.00	268.0	2.73	0.21
Yalcin [51]	BR-S1	550	550	482	1485	300	2.0	445	0.10	425	44.8	0.13	1.00	578.0	2.39	0.13
Hirosawa [52]	43	200	200	173	500	100	2.0	434	0.28	558	19.6	0.10	0.91	73.8	2.54	0.39
	44	200	200	173	500	100	2.0	434	0.28	558	19.6	0.10	0.97	76.5	2.48	0.38
	45	200	200	173	500	100	2.0	434	0.28	558	19.6	0.20	1.00	82.3	2.57	0.29
	46	200	200	173	500	100	2.0	434	0.28	558	19.6	0.20	1.00	80.5	2.52	0.28
	62	200	200	173	500	100	2.0	348	0.28	476	19.6	0.10	0.93	57.8	1.93	0.27
	63	200	200	173	500	100	2.0	348	0.28	476	19.6	0.20	0.86	68.5	2.49	0.27
	64	200	200	173	500	100	2.0	348	0.28	476	19.6	0.20	0.95	68.5	2.25	0.23
Hirosawa [52]	205	200	200	180	600	100	2.0	462	0.28	324	17.7	0.22	0.96	71.2	2.32	0.26
	207	200	200	180	400	100	2.0	462	0.28	324	17.7	0.22	1.00	105.9	3.31	0.45
	208	200	200	180	400	100	2.0	462	0.28	324	17.7	0.55	0.93	135.2	4.56	0.43
	214	200	200	180	600	200	2.0	462	0.14	324	17.7	0.55	1.00	82.7	2.58	0.15
	220	200	200	180	400	120	1.0	379	0.11	648	32.9	0.12	0.75	78.3	3.27	0.32
	231	200	200	180	400	100	1.0	324	0.13	524	14.8	0.26	0.85	50.7	1.87	0.20
	232	200	200	180	400	100	1.0	324	0.13	524	13.1	0.30	0.91	58.3	1.99	0.23
	233	200	200	180	400	100	1.0	372	0.13	524	13.9	0.28	0.81	68.9	2.65	0.36
	234	200	200	180	400	100	1.0	372	0.13	524	13.1	0.30	0.75	67.2	2.80	0.40
Xiao and Martirossyan [53]	HC4-8LI6-T6-0.1P	254	254	222	508	51	2.5	510	0.74	449	86.0	0.10	0.78	273.0	6.83	0.41
	HC4-8L16-T6-0.2P	254	254	222	508	51	2.5	510	0.74	449	86.0	0.19	0.89	324.0	7.07	0.28
Wight James and Sozen Mete [20]	3E	152	305	254	876	127	2.4	496	0.32	345	34.7	0.12	0.93	94.0	2.73	0.23
	3W	152	305	254	876	127	2.4	496	0.32	345	34.7	0.12	0.92	98.0	2.87	0.25
	8E	152	305	254	876	89	2.4	496	0.46	345	26.1	0.15	0.86	101.0	3.18	0.35
	8W	152	305	254	876	89	2.4	496	0.46	345	26.1	0.15	0.82	95.0	3.11	0.34
	3E	152	305	254	876	127	2.4	496	0.32	345	33.6	0.12	0.95	91.0	2.59	0.22
	3W	152	305	254	876	127	2.4	496	0.32	345	33.6	0.12	0.93	101.0	2.91	0.26
	3E	152	305	254	876	127	2.4	496	0.32	345	33.6	0.07	0.96	85.0	2.38	0.25
	3W	152	305	254	876	127	2.4	496	0.32	345	33.6	0.07	0.98	91.0	2.51	0.27
	7E	152	305	254	876	64	2.4	496	0.64	345	33.4	0.11	0.78	86.0	2.96	0.28
	7W	152	305	254	876	64	2.4	496	0.64	345	33.4	0.11	0.81	92.0	3.07	0.29
	2E	152	305	254	876	102	2.4	496	0.91	345	33.5	0.11	0.75	108.0	3.89	0.42
	2W	152	305	254	876	102	2.4	496	0.91	345	33.5	0.11	0.79	113.0	3.87	0.41
Yoshimura [54]	N18M	300	300	255	450	100	2.7	380	0.21	375	26.5	0.18	0.92	263.0	3.96	0.43

	N18C	300	300	255	450	100	2.7	380	0.21	375	26.5	0.18	0.85	264.0	4.34	0.50
	N27M	300	300	255	450	100	2.7	380	0.21	375	26.5	0.27	0.80	288.0	4.98	0.50
	N27C	300	300	255	450	100	2.7	380	0.21	375	26.5	0.27	0.97	263.0	3.76	0.31
	2M	300	300	255	300	100	2.7	396	0.21	392	25.2	0.19	0.78	234.0	4.18	0.48
	2C	300	300	255	300	100	2.7	396	0.21	392	25.2	0.19	0.70	222.0	4.40	0.52
	3M	300	300	255	300	100	2.7	396	0.21	392	25.2	0.28	0.74	248.0	4.63	0.46
	3C	300	300	255	300	100	2.7	396	0.21	392	25.2	0.28	0.72	264.0	5.10	0.53
	2M13	300	300	255	300	100	1.7	350	0.21	392	25.2	0.19	0.92	250.0	3.78	0.41
	2C13	300	300	255	300	100	1.7	350	0.21	392	25.2	0.19	0.79	260.0	4.56	0.55
Yoshimura et al. [55]	No.1	300	300	255	600	100	2.7	402	0.21	392	30.7	0.20	0.95	234.0	3.41	0.27
	No.2	300	300	255	600	150	2.7	402	0.14	392	30.7	0.20	0.95	230.0	3.36	0.27
	No.3	300	300	255	600	200	2.7	402	0.11	392	30.7	0.20	0.96	230.0	3.33	0.26
	No.4	300	300	255	600	100	2.7	402	0.21	392	30.7	0.30	0.96	261.0	3.78	0.24
	No.5	300	300	255	600	100	2.7	402	0.21	392	30.7	0.35	0.81	275.0	4.72	0.32
	No.6	300	300	255	600	100	1.7	409	0.21	392	30.7	0.20	0.85	219.0	3.56	0.29
	No.7	300	300	255	600	150	1.7	409	0.14	392	30.7	0.20	0.90	213.0	3.31	0.26
Nakamura and Yoshimura [56]	C13-J	300	300	255	450	200	1.7	371	0.11	366	22.0	0.20	1.00	191.0	2.65	0.27
	C13-T	300	300	255	450	200	1.7	371	0.11	366	22.0	0.20	1.00	201.0	2.79	0.29
	C13-H	300	300	255	450	200	1.7	371	0.11	366	22.0	0.20	1.00	212.0	2.94	0.31
	4J11	450	450	390	750	300	1.7	403	0.11	360	19.5	0.17	1.00	413.0	2.55	0.31
	4W11	450	450	390	750	300	1.7	403	0.11	360	19.5	0.17	1.00	432.0	2.67	0.34
	4H11	450	450	390	750	300	1.7	403	0.11	360	19.5	0.17	1.00	395.0	2.44	0.29
	6J11	450	450	390	750	300	1.7	403	0.11	360	19.5	0.17	1.00	436.0	2.69	0.34
	4J21	450	450	390	750	150	1.7	403	0.21	360	19.5	0.17	1.00	447.0	2.76	0.35
	4W21	450	450	390	750	150	1.7	403	0.21	360	19.5	0.17	1.00	429.0	2.65	0.33
	6J21	450	450	390	750	150	1.7	403	0.21	360	19.5	0.17	1.00	434.0	2.68	0.34
Nakamura and Yoshimura [57]	A1	450	450	390	450	300	1.1	383	0.11	399	28.0	0.16	1.00	570.0	3.52	0.36
	A2	450	450	390	450	300	1.1	383	0.11	399	28.0	0.16	1.00	557.0	3.44	0.35
	B1	450	450	390	450	150	1.7	383	0.21	399	28.0	0.16	1.00	594.0	3.67	0.39
	B2	450	450	390	450	150	1.7	383	0.21	399	28.0	0.16	1.00	607.0	3.75	0.40
	B3	450	450	390	450	150	1.7	383	0.21	399	28.0	0.16	1.00	545.0	3.36	0.34
	B4	450	450	390	450	150	1.7	383	0.21	399	28.0	0.16	1.00	578.0	3.57	0.37
	B5	450	450	390	450	150	1.7	383	0.21	399	28.0	0.16	1.00	565.0	3.49	0.36
	C1	450	450	390	450	75	2.3	376	0.42	399	28.0	0.16	1.00	687.0	4.24	0.48
	C2	450	450	390	450	75	2.3	376	0.42	399	28.0	0.16	1.00	715.0	4.41	0.51
	S100	450	450	390	450	150	1.7	383	0.21	399	25.0	0.18	1.00	522.0	3.22	0.34
	S60	450	450	390	450	150	1.7	383	0.21	399	25.0	0.18	1.00	577.0	3.56	0.39
	S40	450	450	390	450	150	1.7	383	0.21	399	25.0	0.18	1.00	505.0	3.12	0.32
	S20	450	450	390	450	150	1.7	383	0.21	399	25.0	0.18	1.00	562.0	3.47	0.38
	L100	450	450	390	700	200	1.7	383	0.16	399	25.0	0.18	1.00	506.0	3.12	0.32
	L75	450	450	390	700	200	1.7	383	0.16	399	25.0	0.18	1.00	526.0	3.25	0.34
	L50	450	450	390	700	200	1.7	383	0.16	399	25.0	0.18	1.00	497.0	3.07	0.31
Moretti and Tassios [32]	1	250	250	215	250	50	2.0	480	1.21	300	36.0	0.30	1.00	330.0	6.60	0.52
	3	250	250	215	250	50	4.0	415	1.21	300	39.0	0.30	1.00	360.0	7.20	0.55
	4	250	250	215	250	50	4.0	415	1.21	305	35.0	0.30	1.00	360.0	7.20	0.62
	7	250	250	215	500	50	2.0	480	1.21	300	38.0	0.30	0.91	200.0	4.40	0.24
	8	250	250	215	750	50	2.0	480	1.21	300	38.0	0.30	0.89	140.0	3.13	0.13
Li et al. [58]	1DL	300	500	450	250	100	3.1	438	1.27	430	27.5	0.09	1.00	698.0	5.82	0.90

	1DH	300	500	450	250	100	3.1	438	1.27	430	25.2	0.29	1.00	701.0	5.84	0.64
	1NL	300	500	450	250	200	3.1	438	0.24	458	23.4	0.10	1.00	660.0	5.50	0.92
	1NH	300	500	450	250	200	3.1	438	0.24	458	25.1	0.29	1.00	757.0	6.31	0.73
	2DL	300	500	450	500	100	3.1	438	1.27	430	25.7	0.09	1.00	564.0	4.70	0.73
	2DH	300	500	450	500	100	3.1	438	1.27	430	24.4	0.30	1.00	589.0	4.91	0.50
	1NL	300	500	450	500	200	3.1	438	0.24	458	23.4	0.10	1.00	402.0	3.35	0.49
	2NH	300	500	450	500	200	3.1	438	0.24	458	25.5	0.29	1.00	460.0	3.83	0.32
Ramirez and Jirsa [59]	00-U	305	305	264	458	66	2.5	410	0.32	455	34.5	0.00	0.96	265.9	3.74	0.64
	120C-U	305	305	264	458	66	2.5	410	0.32	455	34.5	0.17	0.95	297.9	4.23	0.38
Bett et al. [60]	SF1	305	305	257	457	210	1.8	462	0.09	414	29.9	0.10	1.00	214.0	2.88	0.31
Hirosawa [52]	372	200	200	170	500	100	1.0	524	0.31	352	20.0	0.30	0.86	74.3	2.70	0.23
	373	200	200	170	500	100	2.0	524	0.31	352	20.4	0.30	0.95	88.1	2.89	0.26
Hirosawa [52]	452	200	200	170	500	100	3.0	524	0.31	352	21.9	0.45	0.99	110.3	3.47	0.24
	454	200	200	170	500	100	4.0	524	0.31	352	21.9	0.45	0.98	110.3	3.50	0.24
Umehara [61]	CUS	230	410	370	455	89	3.0	441	0.28	414	34.9	0.16	1.00	324.0	4.29	0.39
	CUW	410	230	190	455	89	3.0	441	0.31	414	34.9	0.16	1.00	265.0	3.51	0.28
	2CUS	230	410	370	455	89	3.0	441	0.28	414	42.0	0.27	1.00	412.0	5.46	0.34
Ousalem et al. [62]	C1	300	300	260	450	160	1.7	587	0.08	340	13.5	0.30	0.88	160.4	2.54	0.33
	C4	300	300	260	450	75	1.7	384	0.28	340	13.5	0.30	0.81	171.1	2.94	0.42
	C6	300	300	260	450	75	1.7	384	0.28	340	13.5	1.28	0.67	203.9	4.24	0.26
	C8	300	300	260	450	75	1.7	384	0.28	340	18.0	0.30	0.86	233.0	3.77	0.46
	C10	300	300	260	450	75	1.7	384	0.28	340	18.0	1.05	0.81	262.1	4.50	0.24
	C12	300	300	260	450	75	1.7	384	0.28	340	18.0	0.20	0.78	217.1	3.87	0.58
	D1	300	300	260	300	50	1.7	398	0.43	447	27.7	0.22	0.90	341.1	5.24	0.58
	D16	300	300	260	300	50	1.7	398	0.43	447	26.1	0.23	0.89	341.6	5.35	0.61
	D11	300	300	260	450	150	2.3	398	0.14	447	28.2	0.21	0.83	242.8	4.06	0.39
	D12	300	300	260	450	150	2.3	398	0.14	447	28.2	0.21	0.85	250.4	4.09	0.39
	D13	300	300	260	450	50	2.3	398	0.43	447	26.1	0.23	0.83	266.1	4.48	0.47
	D14	300	300	260	450	50	2.3	398	0.43	447	26.1	0.23	0.80	269.1	4.66	0.50
Aboutaha et al. [63]	SC3	914	457	397	1219	407	1.9	434	0.10	400	21.9	0.00	0.99	393.7	1.19	0.25
	SC9	457	914	853	1219	406	1.9	434	0.08	400	21.9	0.00	1.00	587.2	1.76	0.38
Woods [64]	1	457	457	394	1248	457	2.5	445	0.07	372	33.0	0.32	1.00	412.0	2.46	0.09
	2	457	457	394	1248	457	2.5	445	0.07	372	33.0	0.22	1.00	360.0	2.15	0.10
	3	457	457	394	1248	457	3.0	445	0.07	372	33.0	0.32	1.00	313.0	1.87	0.06
Pan and Li [27]	SC-2.4-0.20	350	350	315	850	125	2.1	408	0.13	393	22.6	0.20	1.00	218.9	2.23	0.19
	SC-2.4-0.30	350	350	315	850	125	3.2	409	0.13	393	49.3	0.30	0.97	357.1	3.75	0.13
	SC-2.4-0.50	350	350	315	850	125	2.1	408	0.13	393	24.2	0.50	1.00	237.6	2.43	0.10
	SC-1.7-0.05	350	350	316	600	125	2.1	408	0.13	393	29.8	0.05	1.00	276.4	2.82	0.40
	SC-1.7-0.20	350	350	316	600	125	2.1	408	0.13	393	27.5	0.20	1.00	294.2	3.00	0.25
	SC-1.7-0.35	350	350	316	600	125	2.1	408	0.13	393	25.5	0.35	1.00	335.5	3.42	0.23
	SC-1.7-0.50	350	350	316	600	125	2.1	408	0.13	393	26.4	0.50	1.00	375.6	3.83	0.20
	RC-1.7-0.05	250	490	447	850	125	2.1	408	0.18	393	32.5	0.05	1.00	283.1	2.89	0.38

	RC-1.7-0.20	250	490	447	850	125	2.1	408	0.18	393	24.5	0.20	1.00	305.5	3.12	0.31
	RC-1.7-0.35	250	490	447	850	125	2.1	408	0.18	393	27.1	0.35	1.00	345.7	3.53	0.22
	RC-1.7-0.50	250	490	447	850	125	2.1	408	0.18	393	26.8	0.50	0.99	355.2	3.65	0.18
Boys et al. [65]	24L-300-2D	450	450	412	1624	300	1.0	315	0.12	315	32.0	0.31	0.89	256.4	1.78	0.05
Kogoma et al. [66]	CT1	130	130	99	425	285	4.8	355	0.23	355	22.8	0.18	1.00	24.9	1.84	0.15
Choi et al. [67]	NRC 1	300	300	252	830	300	0.9	327	0.17	378	17.9	0.27	1.00	108.7	1.51	0.10
	NRC 2	300	300	250	830	300	0.9	327	0.17	378	18.3	0.26	1.00	109.1	1.52	0.10
	NRC 3	300	300	250	830	300	1.3	327	0.17	378	17.5	0.28	1.00	116.1	1.61	0.12
	NRC 5	300	300	252	830	300	0.9	327	0.17	378	19.9	0.38	1.00	128.2	1.78	0.09
	NRC 6	300	300	252	630	300	0.9	327	0.17	378	17.2	0.31	0.99	141.1	1.99	0.16
	NRC 7	300	300	249	830	150	1.7	350	0.34	310	12.7	0.31	0.96	122.5	1.78	0.19
	NRC 8	300	300	249	830	150	1.7	350	0.34	310	12.1	0.33	0.95	127.3	1.87	0.21
	NRC 9	300	300	249	830	150	1.7	350	0.34	310	13.0	0.10	0.74	113.1	2.13	0.44
	NRC 10	300	300	249	830	150	1.7	350	0.34	310	13.6	0.44	0.92	140.5	2.11	0.18
Ghannoum Wassim and Moehle Jack [68]	ColA 1	152	152	131	495	102	2.5	552	0.15	655	24.6	0.17	1.00	32.2	1.74	0.13
	ColB 1	152	152	131	495	102	2.5	553	0.15	655	24.6	0.19	1.00	43.9	2.38	0.20
Elwood and Moehle [69]	EL_sp1	229	229	197	737	152	2.5	479	0.18	689	24.5	0.10	1.00	80.5	1.92	0.21
	EL_sp2	229	229	197	737	152	2.5	479	0.18	689	23.9	0.24	1.00	88.1	2.10	0.14

Using the following procedure, the maximum principal tensile stress and the maximum horizontal shear strength were extracted from the experimental specimens:

1. Determination of maximum shear stress:

$$\nu^{exp} = \frac{V^{exp}}{A_e} \times \frac{1}{\lambda} = \frac{V^{exp}}{0.8bh\lambda} \tag{13}$$

in which V^{exp} is the experimental shear capacity; b and h are the width and depth of the column cross-section.

2. Determination of axial stress at a column element using:

$$\bar{\sigma}^{exp} = \frac{N}{bh} \tag{14}$$

in which N is the axial load applied on the column.

$$\sigma_t^{exp} = \sqrt{\left(\frac{\bar{\sigma}^{exp}}{2}\right)^2 + (\nu^{exp})^2} - \frac{\bar{\sigma}^{exp}}{2} \tag{14}$$

Therefore, using the above results, the shear force applied to the member can be converted into the principal tensile stress in the column.

3.2. ANN Model development

An artificial neural network (ANN) was trained to predict the maximum principal tensile stress and corresponding shear strength. Nine input parameters and one normalized output parameter were selected.

The following section explains the rationale for selecting each input and output parameter for the neural network:

1. Parameters b, h, and d: These parameters define the geometry of the laboratory specimen and are provided to the network as input.
2. Parameters ρ_l and f_{yl}: These parameters represent the tensile contribution of the longitudinal reinforcement in the column. Although they have a significant effect on the flexural capacity of the column, their impact on enhancing shear capacity is minimal. However, in shear models [53, 70, 71], these parameters are considered in the determination of the concrete shear

capacity.

3. Parameters s, ρ_t, and f_{yt}: These parameters describe the transverse reinforcement of the column. They play a key and significant role in the shear capacity of the column and also affect the confinement of the concrete core.
4. Parameter a: This represents the distance between the points of maximum and zero moments, known as the shear span, and is provided to the network as an input. In addition to the column's shear span, the angle of diagonal shear cracks in the column depends significantly on this parameter. This parameter is included in shear models [46, 53, 71].
5. Parameter λ: The effect of flexural deformation on the column's shear capacity is indirectly represented by this dimensionless parameter. It should be noted that the experimental shear strength V^{exp} corresponds to μ_Δ. Consequently, the column shear capacity is a function of λ, and this parameter should be considered as an input. However, determining μ_Δ requires section analysis (to determine flexural behavior) and a shear model, whereas the purpose of training the ANN is to predict the shear model itself. Therefore, in this study, V^{exp} corresponding to μ_Δ is converted into shear capacity for $\mu_\Delta < 2$ using Eq. 13. As a result, it is no longer necessary to include this parameter as an input to the ANN.
6. Parameter f'_c: This parameter represents the compressive strength of the concrete, which is a critical property of the column, and is provided to the network as input.
7. Parameter N: The axial load applied to the column is indirectly represented by this parameter. As seen in Eqs. 14 and 15, the effects of this parameter on the column shear capacity are accounted for in $\bar{\sigma}^{exp}$ and σ_t^{exp}.
8. Output parameter $\sigma_t/\sqrt{f'_c}$: The principal tensile stress corresponding to the maximum shear strength at a displacement ductility of less than 2 is normalized by the concrete compressive strength and provided to the network as the output parameter.

Fig. 4 illustrates the architecture of the trained artificial neural network. As shown, this study uses 9 input parameters, 1 output parameter, 20 hidden layers, and 1 output layer for network training. In the ANN modeling, the activation functions in the hidden layers are logarithmic, while the output layer uses a linear activation function. This structure is employed because a single-layer feedforward backpropagation network with bias, a Sigmoid hidden layer, and a linear output layer is capable of approximating any function with a limited number of discontinuities.

In this study, the artificial neural network (ANN) was trained using MATLAB with the trainlm function. The trainlm function is a network training function that updates the weights and biases. Standard backpropagation is a gradient descent algorithm in which the network weights are adjusted along the negative gradient of the performance function. The most commonly used backpropagation training algorithm is the Levenberg–Marquardt algorithm, which has been employed in this study. The dataset used to train the network consists of 164 reinforced concrete column specimens with shear and flexure–shear failure mechanisms. Of these, 70% were randomly assigned for network training, 15% for network validation, and 15% for network testing.

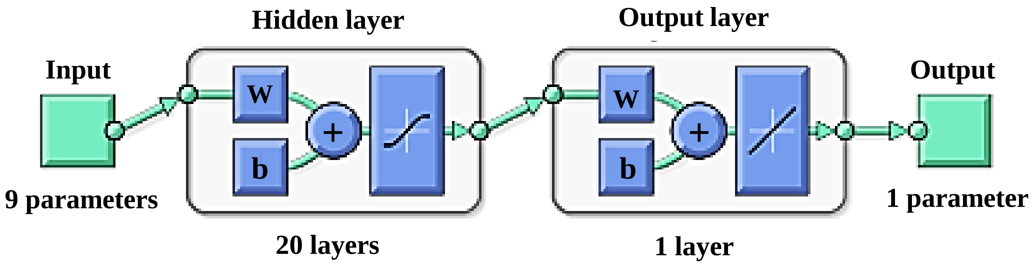

Fig. 4. Architecture of the artificial neural network (ANN) developed for shear strength prediction.

3.3. Model performance and validation

The ANN predictions of principal tensile stress showed close agreement with experimental data. Comparison of predicted and measured values is presented in Fig. 5, while Fig. 6 illustrates the validation against independent test sets. Quantitative results are provided in Table 2, showing mean ratios close to unity and low standard deviations, confirming the reliability of the ANN model.

Table 2. Comparison of shear capacity predictions from ANN and analytical model with experimental results.

ID		f 'c (MPa)	fv (MPa)	$\frac{\sigma_t}{\sqrt{f'_c}}$ (Exp)	$\frac{\sigma_t}{\sqrt{f'_c}}$ (ANN)	$\frac{ANN}{Exp}$	v (Exp)	v (ANN)	$\frac{ANN}{Exp}$	V (Exp)	V (ANN)	$\frac{ANN}{Exp}$
Sezen [2]	1	21.1	3.19	0.19	0.11	0.58	1.90	1.39	0.73	315	229	0.73
	2	21.1	12.8	0.08	0.11	1.48	2.15	2.62	1.22	359	439	1.22
	3	20.9	10.7	0.06	0.11	1.72	1.80	2.39	1.32	301	399	1.32
	4	21.8	3.19	0.17	0.12	0.68	1.80	1.43	0.80	294	234	0.80
Lynn [26]	3CLH18	25.6	2.41	0.16	0.14	0.87	1.63	1.50	0.92	272	250	0.92
	3SLH18	25.6	2.41	0.16	0.14	0.87	1.63	1.50	0.92	273	250	0.92
	2CLH18	33.1	2.41	0.18	0.10	0.58	1.89	1.35	0.71	243	173	0.71
	2SLH18	33.1	2.41	0.12	0.10	0.91	1.43	1.35	0.94	231	218	0.94

	2CMH18	25.7	7.24	0.09	0.09	1.07	1.84	1.91	1.04	308	319	1.04
	3CMH18	27.6	7.24	0.09	0.13	1.42	1.96	2.36	1.21	327	395	1.21
	3CMD12	27.6	7.24	0.11	0.11	0.97	2.13	2.10	0.99	356	351	0.99
	3SMD12	25.7	7.24	0.12	0.12	0.96	2.20	2.15	0.98	367	359	0.98
Ohue et al. [47]	2D16RS	32.1	4.58	0.32	0.33	1.02	3.41	3.45	1.01	102	103	1.01
	4D13RS	29.9	4.58	0.34	0.34	0.97	3.49	3.43	0.98	111	109	0.98
Esaki [48]	H-2-1/5	23.0	4.03	0.47	0.41	0.87	3.79	3.44	0.91	103	94	0.91
	HT-2-1/5	20.2	4.03	0.44	0.44	1.00	3.46	3.47	1.00	102	102	1.00
	H-2-1/3	23.0	6.73	0.37	0.37	0.99	3.88	3.86	0.99	121	120	0.99
	HT-2-1/3	20.2	5.90	0.38	0.42	1.09	3.63	3.82	1.05	112	118	1.05
Li [49]	U-7	29.0	2.90	0.35	0.22	0.63	3.01	2.21	0.73	328	240	0.73
	U-8	33.5	6.70	0.21	0.21	1.01	3.07	3.08	1.00	393	395	1.00
	U-9	34.1	10.23	0.20	0.22	1.09	3.62	3.80	1.05	430	451	1.05
Saatcioglu and Ozcebe [50]	U1	43.6	0.00	0.45	0.18	0.39	2.95	1.16	0.39	275	108	0.39
	U2	30.2	4.90	0.23	0.23	1.02	2.76	2.78	1.01	270	272	1.01
	U3	34.8	4.90	0.21	0.30	1.43	2.73	3.40	1.24	268	334	1.24
Yalcin [51]	BR-S1	44.8	5.95	0.13	0.13	1.01	2.39	2.40	1.01	578	581	1.01
Hirosawa [52]	43	19.6	1.95	0.39	0.34	0.85	2.54	2.27	0.89	74	66	0.89
	44	19.6	1.95	0.38	0.34	0.89	2.48	2.27	0.92	77	70	0.92
	45	19.6	3.90	0.29	0.34	1.17	2.57	2.84	1.10	82	91	1.10
	46	19.6	3.90	0.28	0.34	1.21	2.52	2.84	1.13	81	91	1.13
	62	19.6	1.95	0.27	0.25	0.94	1.93	1.85	0.96	58	55	0.96
	63	19.6	3.90	0.27	0.25	0.92	2.49	2.36	0.95	69	65	0.95
	64	19.6	3.90	0.23	0.25	1.08	2.25	2.36	1.05	69	72	1.05
Hirosawa [52]	205	17.7	3.90	0.26	0.27	1.05	2.32	2.39	1.03	71	73	1.03
	207	17.7	3.90	0.45	0.42	0.93	3.31	3.15	0.95	106	101	0.95
	208	17.7	9.80	0.43	0.42	0.98	4.56	4.50	0.99	135	133	0.99
	214	17.7	9.80	0.15	0.15	0.98	2.58	2.56	0.99	83	82	0.99
	220	32.9	3.90	0.32	0.33	1.01	3.27	3.29	1.01	78	79	1.01
	231	14.8	3.90	0.20	0.20	1.00	1.87	1.88	1.00	51	51	1.00
	232	13.1	3.90	0.23	0.20	0.86	1.99	1.83	0.92	58	53	0.92
	233	13.9	3.90	0.36	0.38	1.05	2.65	2.73	1.03	69	71	1.03
	234	13.1	3.90	0.40	0.38	0.95	2.80	2.71	0.97	67	65	0.97
Xiao and Martirossyan [53]	T6-0.1P	86.0	8.28	0.41	0.42	1.00	6.83	6.83	1.00	273	273	1.00
	T6-0.2P	86.0	16.55	0.28	0.42	1.48	7.07	8.86	1.25	324	406	1.25
Wight James and Sozen Mete [20]	3E	34.7	4.08	0.23	0.24	1.03	2.73	2.77	1.02	94	95	1.02
	3W	34.7	4.08	0.25	0.24	0.95	2.87	2.77	0.97	98	95	0.97
	8E	26.1	3.84	0.35	0.34	0.95	3.18	3.09	0.97	101	98	0.97
	8W	26.1	3.84	0.34	0.34	0.99	3.11	3.09	0.99	95	94	0.99
	3E	33.6	4.08	0.22	0.24	1.12	2.59	2.77	1.07	91	97	1.07
	3W	33.6	4.08	0.26	0.24	0.93	2.91	2.77	0.95	101	96	0.95
	3E	33.6	2.39	0.25	0.24	0.96	2.38	2.31	0.97	85	83	0.97
	3W	33.6	2.39	0.27	0.24	0.88	2.51	2.31	0.92	91	84	0.92
	7E	33.4	3.84	0.28	0.30	1.09	2.96	3.13	1.06	86	91	1.06
	7W	33.4	3.84	0.29	0.30	1.03	3.07	3.13	1.02	92	94	1.02
	2E	33.5	3.84	0.42	0.41	0.99	3.89	3.86	0.99	108	107	0.99
	2W	33.5	3.84	0.41	0.41	1.00	3.87	3.86	1.00	113	113	1.00
Yoshimura [54]	N18M	26.5	4.77	0.43	0.43	0.99	3.96	3.92	0.99	263	261	0.99
	N18C	26.5	4.77	0.50	0.43	0.86	4.34	3.92	0.90	264	239	0.90
	N27M	26.5	7.17	0.50	0.43	0.87	4.98	4.55	0.91	288	263	0.91

	N27C	26.5	7.17	0.31	0.43	1.37	3.76	4.55	1.21	263	318	1.21
	2M	25.2	4.78	0.48	0.48	0.99	4.18	4.14	0.99	234	232	0.99
	2C	25.2	4.78	0.52	0.48	0.91	4.40	4.14	0.94	222	209	0.94
	3M	25.2	7.08	0.46	0.48	1.05	4.63	4.76	1.03	248	255	1.03
	3C	25.2	7.08	0.53	0.48	0.90	5.10	4.76	0.93	264	246	0.93
	2M13	25.2	4.78	0.41	0.41	0.99	3.78	3.75	0.99	250	248	0.99
	2C13	25.2	4.78	0.55	0.41	0.75	4.56	3.75	0.82	260	214	0.82
	No.1	30.7	6.14	0.27	0.29	1.05	3.41	3.50	1.03	234	240	1.03
	No.2	30.7	6.14	0.27	0.25	0.95	3.36	3.26	0.97	230	223	0.97
	No.3	30.7	6.14	0.26	0.22	0.85	3.33	3.02	0.91	230	208	0.91
Yoshimura et al. [55]	No.4	30.7	9.21	0.24	0.29	1.17	3.78	4.14	1.09	261	286	1.09
	No.5	30.7	10.75	0.32	0.29	0.89	4.72	4.42	0.94	275	258	0.94
	No.6	30.7	6.14	0.29	0.30	1.03	3.56	3.63	1.02	219	223	1.02
	No.7	30.7	6.14	0.26	0.25	0.97	3.31	3.24	0.98	213	209	0.98
	C13-J	22.0	4.40	0.27	0.29	1.09	2.65	2.79	1.05	191	201	1.05
	C13-T	22.0	4.40	0.29	0.29	1.00	2.79	2.79	1.00	201	201	1.00
	C13-H	22.0	4.40	0.31	0.29	0.92	2.94	2.79	0.95	212	201	0.95
	4J11	19.5	3.32	0.31	0.32	1.03	2.55	2.60	1.02	413	421	1.02
Nakamura and Yoshimura [56]	4W11	19.5	3.32	0.34	0.32	0.96	2.67	2.60	0.97	432	421	0.97
	4H11	19.5	3.32	0.29	0.32	1.10	2.44	2.60	1.07	395	421	1.07
	6J11	19.5	3.32	0.34	0.32	0.95	2.69	2.60	0.96	436	421	0.96
	4J21	19.5	3.32	0.35	0.33	0.92	2.76	2.62	0.95	447	424	0.95
	4W21	19.5	3.32	0.33	0.33	0.98	2.65	2.62	0.99	429	424	0.99
	6J21	19.5	3.32	0.34	0.33	0.97	2.68	2.62	0.98	434	424	0.98
	A1	28.0	4.48	0.36	0.36	0.98	3.52	3.48	0.99	570	564	0.99
	A2	28.0	4.48	0.35	0.36	1.02	3.44	3.48	1.01	557	564	1.01
	B1	28.0	4.48	0.39	0.37	0.96	3.67	3.58	0.98	594	580	0.98
	B2	28.0	4.48	0.40	0.37	0.93	3.75	3.58	0.95	607	580	0.95
	B3	28.0	4.48	0.34	0.37	1.10	3.36	3.58	1.06	545	580	1.06
	B4	28.0	4.48	0.37	0.37	1.00	3.57	3.58	1.00	578	580	1.00
	B5	28.0	4.48	0.36	0.37	1.04	3.49	3.58	1.03	565	580	1.03
	C1	28.0	4.48	0.48	0.50	1.04	4.24	4.37	1.03	687	708	1.03
Nakamura and Yoshimura [57]	C2	28.0	4.48	0.51	0.50	0.99	4.41	4.37	0.99	715	708	0.99
	S100	25.0	4.50	0.34	0.34	1.02	3.22	3.27	1.01	522	529	1.01
	S60	25.0	4.50	0.39	0.34	0.87	3.56	3.27	0.92	577	529	0.92
	S40	25.0	4.50	0.32	0.34	1.08	3.12	3.27	1.05	505	529	1.05
	S20	25.0	4.50	0.38	0.34	0.91	3.47	3.27	0.94	562	529	0.94
	L100	25.0	4.50	0.32	0.33	1.03	3.12	3.18	1.02	506	516	1.02
	L75	25.0	4.50	0.34	0.33	0.97	3.25	3.18	0.98	526	516	0.98
	L50	25.0	4.50	0.31	0.33	1.06	3.07	3.18	1.04	497	516	1.04
	1	36.0	10.80	0.52	0.41	0.80	6.60	5.75	0.87	330	288	0.87
	3	39.0	11.70	0.55	0.56	1.02	7.20	7.27	1.01	360	363	1.01
Moretti and Tassios [32]	4	35.0	10.50	0.62	0.61	0.98	7.20	7.12	0.99	360	356	0.99
	7	38.0	11.40	0.24	0.20	0.82	4.40	3.94	0.90	200	179	0.90
	8	38.0	11.40	0.13	0.14	1.04	3.13	3.19	1.02	140	143	1.02
	1DL	27.5	2.48	0.90	0.63	0.70	5.82	4.38	0.75	698	525	0.75
	1DH	25.2	7.31	0.64	0.64	1.00	5.84	5.83	1.00	701	699	1.00
Li et al. [58]	1NL	23.4	2.34	0.92	0.72	0.79	5.50	4.52	0.82	660	543	0.82
	1NH	25.1	7.28	0.73	0.72	1.00	6.31	6.29	1.00	757	755	1.00
	2DL	25.7	2.31	0.73	0.61	0.84	4.70	4.09	0.87	564	491	0.87

	2DH	24.4	7.32	0.50	0.62	1.24	4.91	5.62	1.15	589	674	1.15
	1NL	23.4	2.34	0.49	0.31	0.63	3.35	2.40	0.72	402	288	0.72
	2NH	25.5	7.40	0.32	0.32	0.98	3.83	3.79	0.99	460	455	0.99
Ramirez and Jirsa [59]	00-U	34.5	0.00	0.64	0.50	0.79	3.74	2.95	0.79	266	210	0.79
	120C-U	34.5	5.74	0.38	0.50	1.31	4.23	5.06	1.20	298	356	1.20
Bett et al. [60]	SF1	29.9	3.10	0.31	0.32	1.01	2.88	2.89	1.01	214	215	1.01
Hirosawa [52]	372	20.0	6.03	0.23	0.23	1.01	2.70	2.72	1.00	74	75	1.00
	373	20.4	6.03	0.26	0.30	1.16	2.89	3.15	1.09	88	96	1.09
Hirosawa [52]	452	21.9	9.78	0.24	0.24	1.01	3.47	3.48	1.00	110	111	1.00
	454	21.9	9.78	0.24	0.24	1.01	3.50	3.52	1.01	110	111	1.01
Umehara [61]	CUS	34.9	5.66	0.39	0.27	0.70	4.29	3.42	0.80	324	258	0.80
	CUW	34.9	5.66	0.28	0.28	0.99	3.51	3.48	0.99	265	263	0.99
	2CUS	42.0	11.33	0.34	0.35	1.02	5.46	5.53	1.01	412	417	1.01
Ousalem et al. [62]	C1	13.5	4.05	0.33	0.34	1.01	2.54	2.56	1.01	160	161	1.01
	C4	13.5	4.05	0.42	0.34	0.80	2.94	2.56	0.87	171	149	0.87
	C6	13.5	17.26	0.26	0.34	1.30	4.24	4.78	1.13	204	230	1.13
	C8	18.0	5.40	0.46	0.35	0.77	3.77	3.20	0.85	233	198	0.85
	C10	18.0	18.89	0.24	0.35	1.47	4.50	5.51	1.23	262	321	1.23
	C12	18.0	3.60	0.58	0.35	0.60	3.87	2.75	0.71	217	155	0.71
	D1	27.7	6.00	0.58	0.59	1.03	5.24	5.33	1.02	341	347	1.02
	D16	26.1	6.00	0.61	0.60	0.98	5.35	5.26	0.98	342	336	0.98
	D11	28.2	6.00	0.39	0.38	0.99	4.06	4.02	0.99	243	241	0.99
	D12	28.2	6.00	0.39	0.38	0.97	4.09	4.02	0.98	250	246	0.98
	D13	26.1	6.00	0.47	0.50	1.06	4.48	4.65	1.04	266	276	1.04
	D14	26.1	6.00	0.50	0.50	1.00	4.66	4.65	1.00	269	269	1.00
Aboutaha et al. [63]	SC3	21.9	0.00	0.25	0.25	0.99	1.19	1.18	0.99	394	390	0.99
	SC9	21.9	0.00	0.38	0.37	0.99	1.76	1.74	0.99	587	582	0.99
Woods [64]	1	33.0	10.64	0.09	0.10	1.04	2.46	2.51	1.02	412	420	1.02
	2	33.0	7.24	0.10	0.10	0.95	2.15	2.10	0.97	360	351	0.97
	3	33.0	10.64	0.06	0.06	1.04	1.87	1.91	1.02	313	319	1.02
Pan and Li [27]	SC-2.4-0.20	22.6	4.52	0.19	0.13	0.65	2.23	1.75	0.78	219	172	0.78
	SC-2.4-0.30	49.3	14.79	0.13	0.13	0.99	3.75	3.74	1.00	357	356	1.00
	SC-2.4-0.50	24.2	12.10	0.10	0.14	1.50	2.43	3.00	1.23	238	293	1.23
	SC-1.7-0.05	29.8	1.49	0.40	0.31	0.78	2.82	2.31	0.82	276	227	0.82
	SC-1.7-0.20	27.5	5.50	0.25	0.28	1.10	3.00	3.18	1.06	294	312	1.06
	SC-1.7-0.35	25.5	8.93	0.23	0.25	1.10	3.42	3.61	1.05	336	354	1.05
	SC-1.7-0.50	26.4	13.20	0.20	0.26	1.31	3.83	4.44	1.16	376	435	1.16
	RC-1.7-0.05	32.5	1.63	0.38	0.34	0.88	2.89	2.63	0.91	283	257	0.91
	RC-1.7-0.20	24.5	4.90	0.31	0.24	0.78	3.12	2.68	0.86	306	262	0.86
	RC-1.7-0.35	27.1	9.49	0.22	0.27	1.20	3.53	3.90	1.11	346	382	1.11
	RC-1.7-0.50	26.8	13.40	0.18	0.26	1.47	3.65	4.50	1.23	355	437	1.23
Boys et al. [65]	24L-300-2D	32.0	9.88	0.05	0.06	1.04	1.78	1.81	1.02	256	261	1.02
Kogoma et al. [66]	SF1	22.8	4.10	0.15	0.15	1.02	1.84	1.86	1.01	25	25	1.01
Choi et al. [67]	NRC 1	17.9	4.83	0.10	0.10	0.96	1.51	1.48	0.98	109	107	0.98
	NRC 2	18.3	4.76	0.10	0.09	0.92	1.52	1.44	0.95	109	104	0.95
	NRC 3	17.5	4.90	0.12	0.12	1.05	1.61	1.65	1.03	116	119	1.03
	NRC 5	19.9	7.56	0.09	0.08	0.91	1.78	1.69	0.95	128	122	0.95
	NRC 6	17.2	5.33	0.16	0.17	1.06	1.99	2.05	1.03	141	145	1.03
	NRC 7	12.7	3.94	0.19	0.25	1.32	1.78	2.09	1.17	122	144	1.17
	NRC 8	12.1	3.99	0.21	0.25	1.20	1.87	2.07	1.11	127	141	1.11

	NRC 9	13.0	1.30	0.44	0.25	0.58	2.13	1.42	0.67	113	76	0.67
	NRC 10	13.6	5.98	0.18	0.25	1.39	2.11	2.55	1.20	140	169	1.20
Ghannoum Wassim and Moehle Jack [68]	ColA1	24.6	4.18	0.13	0.13	1.01	1.74	1.76	1.01	32	32	1.01
	ColB1	24.6	4.67	0.20	0.13	0.65	2.38	1.85	0.78	44	34	0.78
Elwood and Moehle [69]	EL_sp1	24.5	2.45	0.21	0.21	1.00	1.92	1.92	1.00	81	81	1.00
	EL_sp2	23.9	5.74	0.14	0.21	1.52	2.10	2.66	1.27	88	112	1.27
					Mean	0.997		Mean	0.988		Mean	0.988
					SD	0.191		SD	0.120		SD	0.120

Fig. 5 compares the principal tensile stress $\sigma_t/\sqrt{f'_c}$: predicted by the ANN with the experimental results. Among the 114 samples randomly selected for network training, in more than 85 samples, the difference between the principal tensile stress predicted by the ANN and the laboratory results is less than 0.005. For the remaining training samples, the network prediction accuracy is still considered acceptable. The maximum difference in these training samples is 0.261. Among the 25 samples selected for network validation, only 4 samples exhibited a difference between the principal tensile stress $\sigma_t/\sqrt{f'_c}$: predicted by the ANN and the experimental results greater than 0.1, with the maximum difference being 0.261. Similarly, of the 25 samples selected for network testing, only 3 column specimens showed a difference between the principal tensile stress $\sigma_t/\sqrt{f'_c}$: predicted by the ANN and the experimental results exceeding 0.1. The maximum difference in these samples is 0.18. As a result, it can be concluded that the trained artificial neural network (ANN) predicts the experimental results with satisfactory accuracy.

Fig. 6 compares the results predicted by the trained ANN with the experimental data. It should be noted that another factor for selecting an appropriate network is the regression coefficient (R) of the network. The regression coefficient measures the correlation between the outputs and targets in an ANN, where R = 1 indicates a perfect correlation, and R = 0 indicates a random relationship. As shown previously, the ANN predicts the experimental results with high accuracy, and this figure demonstrates the consistency of the predictions across all training, validation, and test samples.

Table 2 compares the responses of the experimental column specimens in terms of principal tensile stress, shear strength, and shear force with the results from the ANN and the analytical model. As observed, the experimental column responses in terms of principal tensile stress are predicted by the ANN with a mean value of 0.997 and a standard deviation of 0.191, confirming an accurate and nearly uniform prediction of the column behavior. Using Eq. 12, the principal tensile stress can be converted to the horizontal shear capacity. The mean value of 0.988 and standard deviation of 0.120 indicate a more uniform prediction of shear strength compared to principal tensile stress. The column shear strength can be further converted into the column shear force using Eq. 10. Finally, considering the mean value of 0.988 and standard deviation of 0.120, it can be concluded that the trained ANN, combined with theoretical relationships, can accurately and consistently predict the column shear force. The capability of the proposed model will next be compared with other shear models presented in the literature.

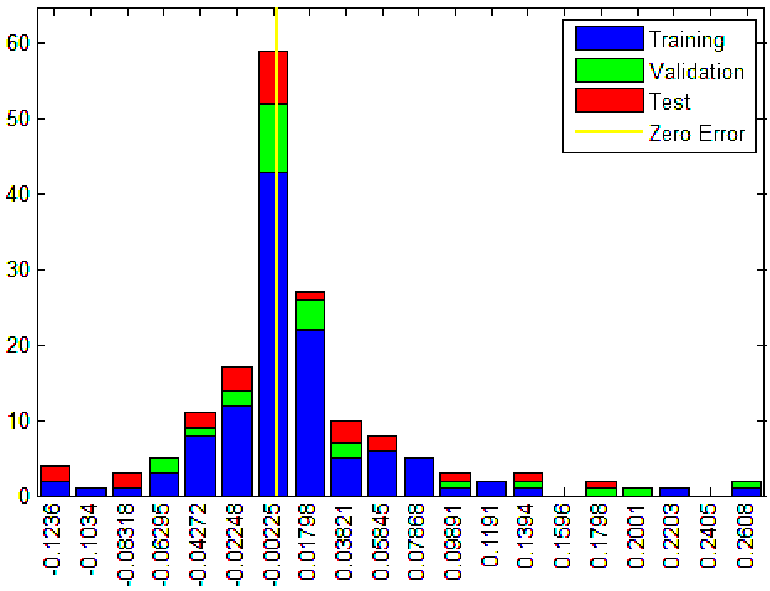

Fig. 5. Comparison of principal tensile stress predicted by the ANN with experimental results for training specimens. The vertical axis represents predicted values from the ANN, while the horizontal axis represents experimental values.

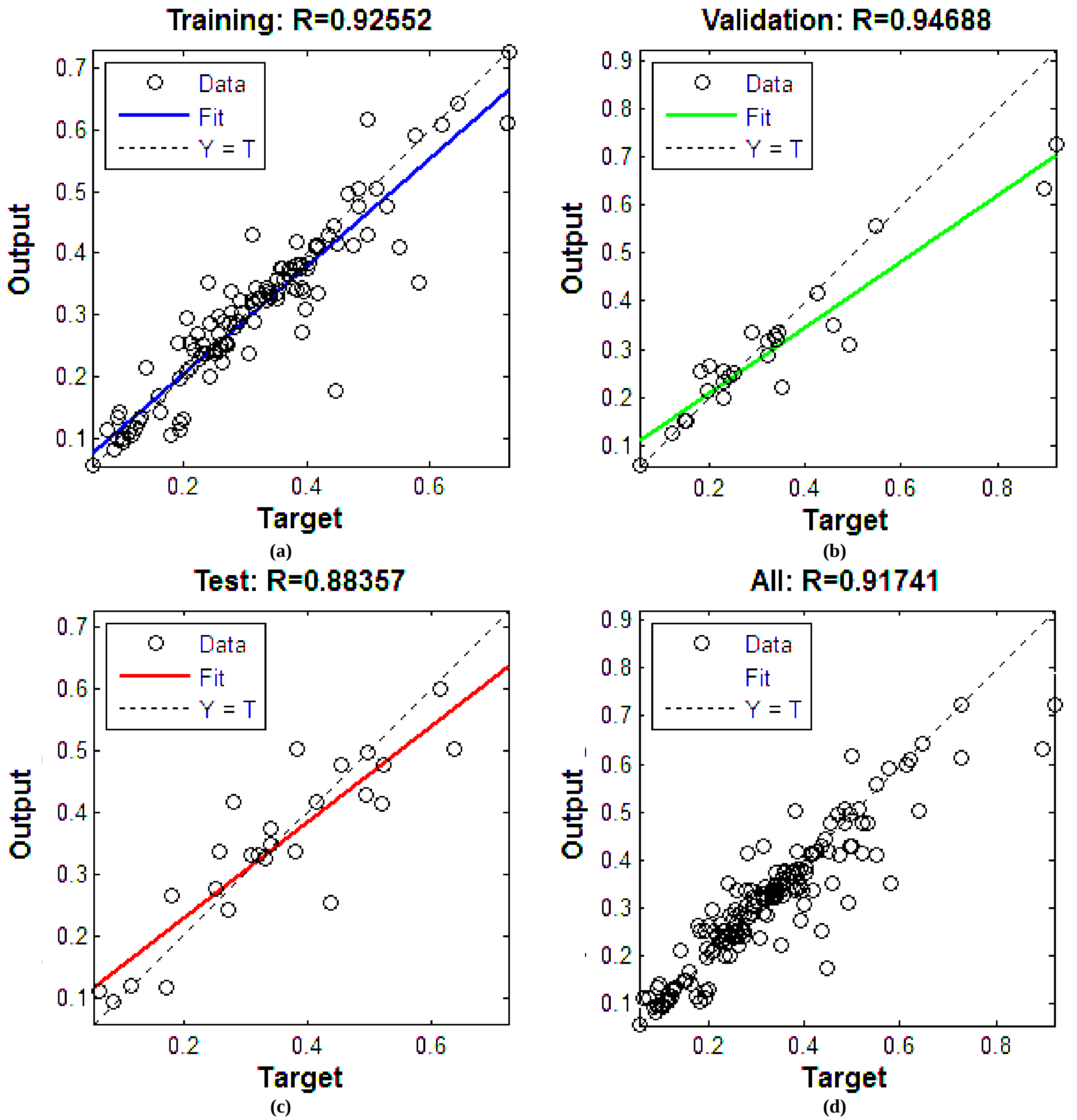

Fig. 6. Predictive performance for the proposed ANN model based on: a) data used for training; b) data used for validation; c) data used for testing; d) all data.

3.4. Comparison with existing models

The proposed ANN-based shear model was benchmarked against existing analytical shear strength models in the literature [22, 23, 46, 53, 70-73]. As shown in Fig. 7, an evaluation of the mean values and coefficients of variation indicates that the artificial neural network (ANN) model predicts the experimental results with a higher degree of consistency and accuracy compared to other existing models (see Table 2). The ANN model not only captures the central tendency of the experimental data but also demonstrates reduced scatter in its predictions, which reflects a more reliable representation of the reinforced concrete columns' behavior under shear-dominated loading conditions. It is worth noting that the shear model proposed by Sezen and Moehle Jack [46], with a mean value of 1.083 and a coefficient of variation of 0.252, performs better than other traditional shear models in terms of both accuracy and uniformity of predictions. However, when compared to the ANN model, the proposed approach offers an even more consistent performance across the entire dataset, reducing variability and providing improved predictive reliability. Based on this comparative assessment, it can be concluded that the proposed ANN-based model demonstrates satisfactory reliability in predicting the behavior of reinforced concrete columns subjected to shear forces. Its ability to consistently approximate both the peak response and the overall trend of experimental results highlights its potential as a robust and practical tool for structural analysis and design, particularly in situations where accurate estimation of shear capacity and post-peak behavior is critical.

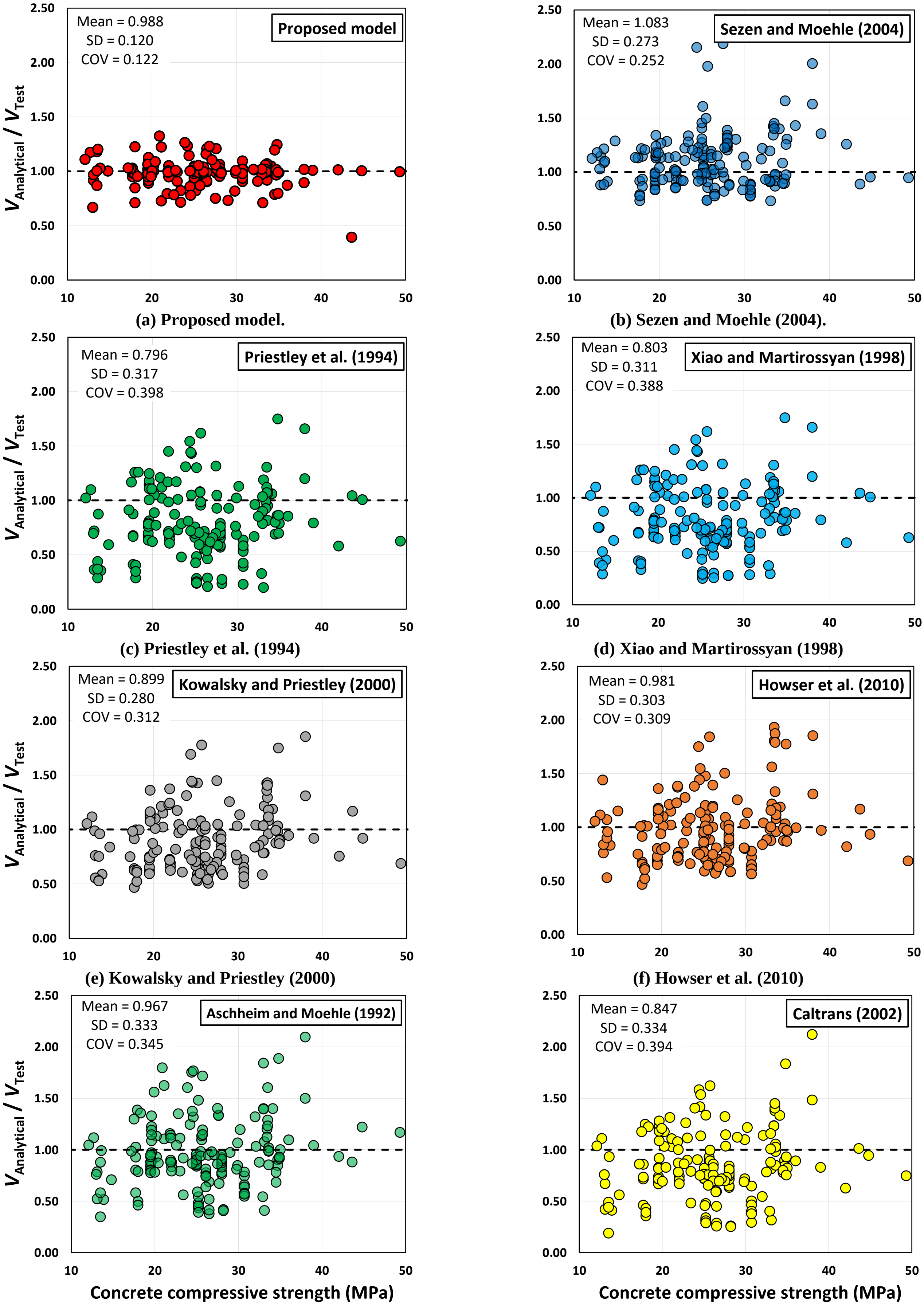

(a) Proposed model.

(b) Sezen and Moehle (2004).

(c) Priestley et al. (1994)

(d) Xiao and Martirossyan (1998)

(e) Kowalsky and Priestley (2000)

(f) Howser et al. (2010)

(g) Aschheim and Moehle (1992)

(h) Caltrans (2002)

Fig. 7. Comparison of shear strength predictions from the proposed ANN model with existing analytical models and experimental results [22, 23, 46, 53, 70-73].

Fig. 8 illustrates the validation of the proposed model against the experimental results reported by Lynn [26], focusing on the load-displacement behavior of reinforced concrete columns up to the point of shear failure. In this study, the shear capacity of the columns was evaluated using the proposed analytical model, which incorporates the governing equations, underlying assumptions, and numerical implementation described in the preceding sections. The flexural response, on the other hand, was obtained through a moment–curvature analysis based on the lumped plastic hinge concept. This approach allows the nonlinear flexural behavior to be represented by concentrated rotation at the member ends, while maintaining linear elasticity along the remaining length. The resulting moment–curvature relationships were subsequently converted into load–displacement responses by defining the hinge locations and their corresponding rotational capacities. This combined modeling framework enables a consistent and accurate representation of both shear- and flexure-dominated behaviors in reinforced concrete columns. As shown in Fig. 8, the simulated load–displacement curves generated by the proposed model closely follow the experimental data across the entire range, from the initial elastic response to the post-peak behavior. This close agreement demonstrates the model's capability to accurately capture key structural characteristics, including the initial stiffness, peak load, and post-peak ductility of the columns, which are critical for evaluating the performance of reinforced concrete members subjected to shear-dominated failure modes. Notably, while specimen 2CMH18 exhibited a predominantly flexural failure mode in the experiments, the proposed model was still able to replicate its response with a high degree of accuracy. Specifically, the model successfully predicted the strength, the initial stiffness of the member, and its overall ductility, highlighting the robustness of the modeling approach in capturing both shear- and flexure-dominated behaviors. By contrast, the Sezen and Moehle Jack [46] model provides a more conservative estimate of the experimental results. The predicted peak load is approximately 50% lower than the observed experimental values, and the location of failure is estimated within the elastic range of the load–displacement curve, rather than near the actual failure point observed in the experiments. This discrepancy indicates that, although the Sezen and Moehle Jack [46] model can offer a safe conservative assessment, it does not accurately capture the actual behavior of reinforced concrete columns under shear-dominated failure. Overall, the comparison highlights that the proposed model not only predicts the peak strength with higher accuracy but also provides a more realistic representation of the entire load–displacement response. This demonstrates the model's effectiveness as a predictive tool for reinforced concrete columns, particularly in post-fire or retrofitted scenarios where accurate evaluation of both shear and flexural responses is essential for structural safety and reliability.

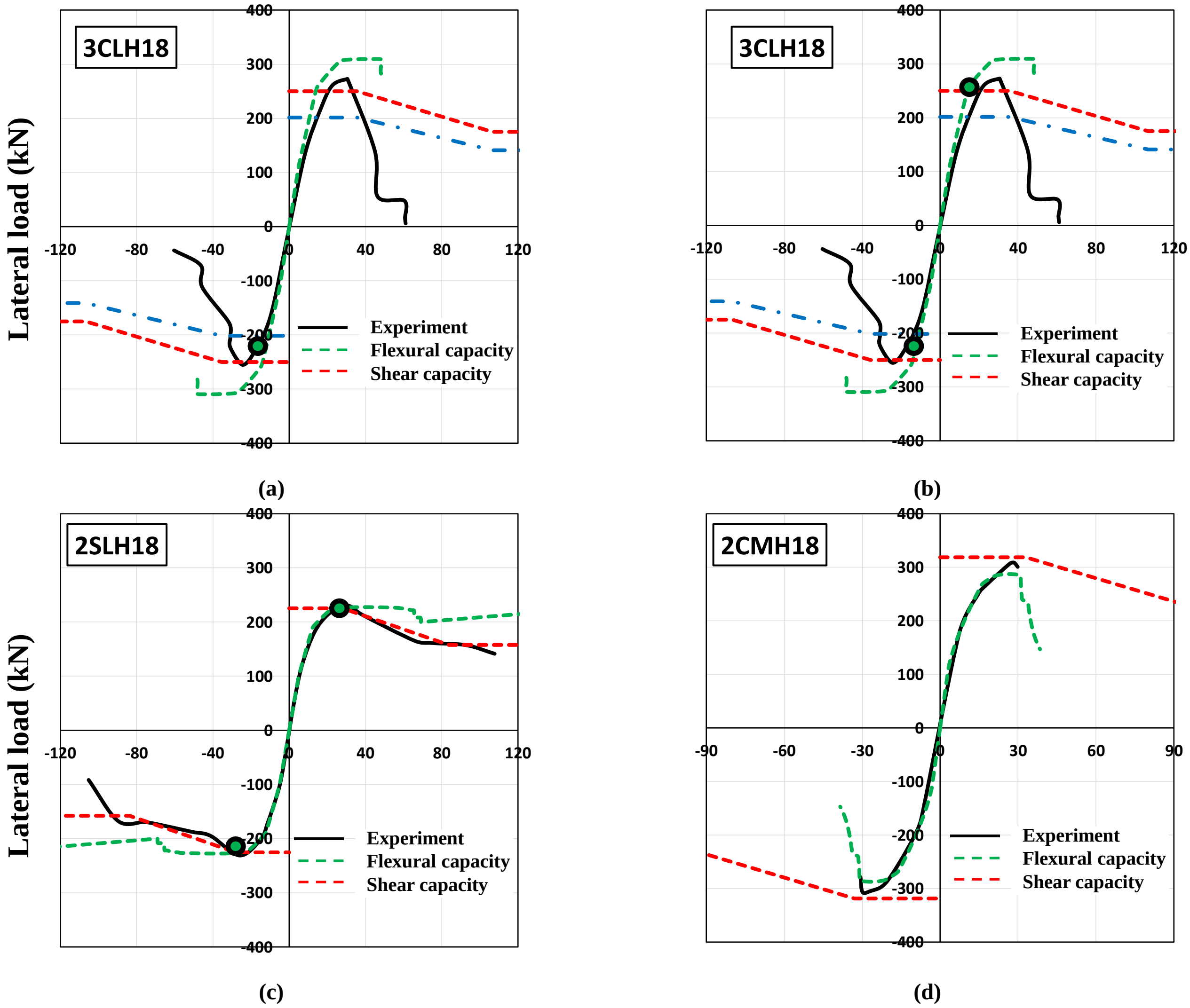

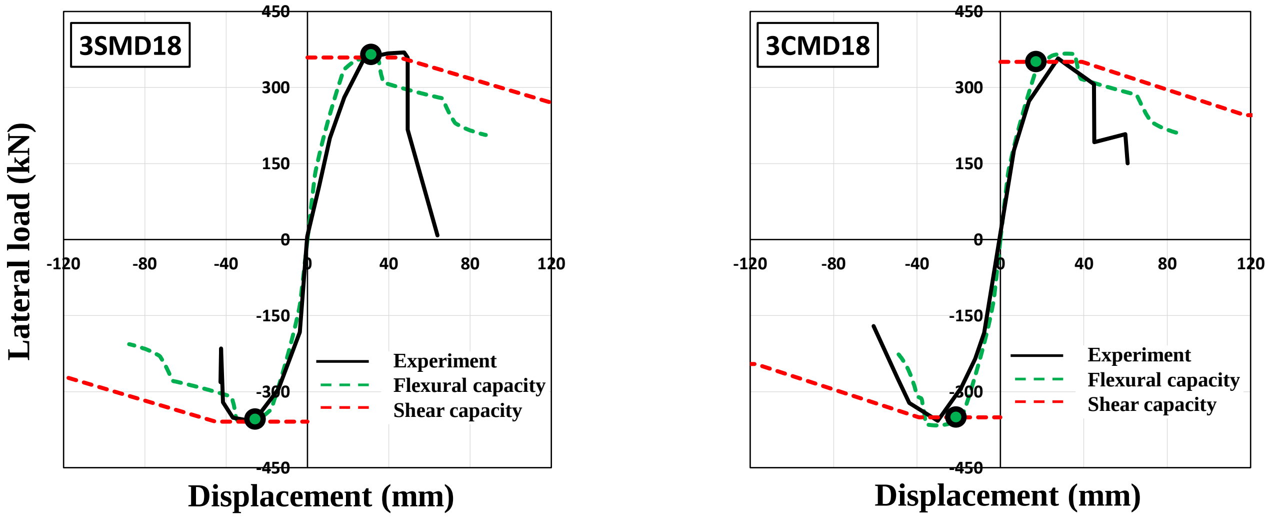

(e) (f)

Fig. 8. Validation of the proposed ANN model against experimental load–displacement responses of RC columns [26].

4. Conclusion

This study investigated the nonlinear flexural–shear behavior of reinforced concrete (RC) columns designed according to older seismic codes, which often exhibit insufficient shear capacity and are vulnerable to brittle shear or flexure–shear failures during seismic events. The key contributions and findings of this research are summarized below:

- A comprehensive shear model was developed based on Mohr's circle, incorporating both compressive and tensile principal stress surfaces. The model was further extended to capture the degradation of shear capacity as a function of flexural deformations through a displacement ductility-dependent parameter, enabling a more realistic representation of the shear behavior under seismic loading.

- An artificial neural network (ANN) was trained using a database of 164 RC column specimens exhibiting shear or flexure–shear failure modes. The ANN effectively learned the nonlinear interaction between geometric, material, and loading parameters, accurately predicting the principal tensile stress and shear strength. The model demonstrated high accuracy and uniformity across training, validation, and testing datasets.

- When compared with existing analytical models available in the literature, the ANN-based model provided more consistent and reliable predictions of shear strength. Statistical analyses of mean values and coefficients of variation confirmed the superior performance of the proposed model in replicating experimental observations.

Overall, the proposed framework, which combines analytical modeling with data-driven ANN approaches, provides a robust and accurate tool for predicting the nonlinear shear response of RC columns. This can support more reliable seismic assessment and retrofit strategies for existing structures designed according to outdated seismic codes.

Statements & Declarations

Author contributions

Maedeh Sadeghpour Haji: Project administration, Resources, Writing – Review & Editing.

Reza Niknam: Investigation, Formal analysis, Data curation, Software, Writing – Original Draft.

Javad Shayanfar: Conceptualization, Methodology, Software, Writing – Review & Editing.

Funding

The authors received no financial support for the research, authorship, and/or publication of this article.

Data availability

The data presented in this study will be available on interested request from the corresponding author.

Declarations

The authors declare no conflict of interes.

References

[1] Steinbrugge, K. V. NISEE e-Library, The Earthquake Engineering Online Archive. 1964. Available online: https://nisee.berkeley.edu/elibrary/search?in=0&ss=Steinbrugge&start=571 (accessed on December 2025).

[2] Sezen, H. Seismic behavior and modeling of reinforced concrete building columns (PhD Thesis). Berkeley (CA): University of California Berkley; 2002.

[3] Shayanfar, J., Akbarzadeh Bengar, H. Nonlinear analysis of RC frames considering shear behaviour of members under varying axial load. Bulletin of Earthquake Engineering, 2017; 15: 2055-2078. doi:10.1007/s10518-016-0060-z.

[4] Shayanfar, J., Bengar, H. A., Parvin, A. Analytical prediction of seismic behavior of RC joints and columns under varying axial load. Engineering Structures, 2018; 174: 792-813. doi:10.1016/j.engstruct.2018.07.103.

[5] Shayanfar, J., Hemmati, A., Bengar, H. A. A simplified numerical model to simulate RC beam–column joints collapse. Bulletin of Earthquake Engineering, 2019; 17: 803-844. doi:10.1007/s10518-018-0472-z.

[6] Shayanfar, J., Bengar, H. A. Numerical model to simulate shear behaviour of RC joints and columns. Computers and Concrete, An International Journal, 2016; 18: 877-901. doi:10.12989/cac.2016.18.4.877.

[7] Shayanfar, J., Akbarzadeh Bengar, H., Niroomandi, A. A proposed model for predicting nonlinear behavior of RC joints under seismic loads. Materials & Design, 2016; 95: 563-579. doi:10.1016/j.matdes.2016.01.098.

[8] John, S. K., Cascardi, A., Verre, S., Nadir, Y. RC-columns subjected to lateral cyclic force with different FRCM-strengthening schemes: experimental and numerical investigation. Bulletin of Earthquake Engineering, 2025; 23: 1561-1590. doi:10.1007/s10518-025-02100-5.

[9] Shayanfar, J., Barros Joaquim, A. O., Rezazadeh, M. Stress–Strain Model for FRP-Confined Circular Concrete Columns Developing Structural Softening Behavior. Journal of Composites for Construction, 2024; 28: 04023065. doi:10.1061/JCCOF2.CCENG-4364.

[10] Işık, E., Radu, D., Harirchian, E., Avcil, F., Arkan, E., Büyüksaraç, A., Hadzima-Nyarko, M. Failures in Reinforced-Concrete Columns and Proposals for Reinforcement Solutions: Insights from the 2023 Kahramanmaraş Earthquakes. Buildings, 2025; 15: 1535.

[11] Nematzadeh, M., Mousavimehr, M., Shayanfar, J., Omidalizadeh, M. Eccentric compressive behavior of steel fiber-reinforced RC columns strengthened with CFRP wraps: Experimental investigation and analytical modeling. Engineering Structures, 2021; 226: 111389. doi:10.1016/j.engstruct.2020.111389.

[12] Shayanfar, J., Barros, J. A. O., Rezazadeh, M. Analytical model to predict axial stress-strain behavior of heat-damaged unreinforced concrete columns wrapped by FRP jacket. Engineering Structures, 2023; 289: 116244. doi:10.1016/j.engstruct.2023.116244.

[13] Wang, J., Xiao, H., Lu, L., Yang, J., Lu, S., Shayanfar, J. Axial stress-strain model for concrete in partially FRP wrapped reinforced concrete columns. Construction and Building Materials, 2024; 416: 135028. doi:10.1016/j.conbuildmat.2024.135028.

[14] Shayanfar, J., Barros Joaquim, A. O., Abedi, M., Rezazadeh, M. Unified Compressive Strength and Strain Ductility Models for Fully and Partially FRP-Confined Circular, Square, and Rectangular Concrete Columns. Journal of Composites for Construction, 2023; 27: 04023053. doi:10.1061/JCCOF2.CCENG-4336.

[15] Zhao, Y., Zhang, X., Zhuang, X. Seismic performance of squared lap-spliced RC columns strengthened by active confinement technique under quasi-static cyclic load. Structures, 2025; 74: 108622. doi:10.1016/j.istruc.2025.108622.

[16] Shayanfar, J., Barros, J. A. O., Rezazadeh, M. Cross-sectional and confining system unification on peak compressive strength of FRP confined concrete. Structural Concrete, 2023; 24: 1531-1545. doi:10.1002/suco.202200105.

[17] Baldwin, J., Viest, I. Effect of Axial Compression on Shear Strength of Reinforced Concrete Frame Members. ACI Journal Proceedings, 1958; 55: 635-654. doi:10.14359/11379.

[18] Yamad, M. Shear Strength, Deformation and Explosion of Reinforced Concrete Short Columns. American Concrete Institute (ACI), 1974; 42: 617-640. doi:10.14359/17304.

[19] Elzanaty, A. H., Nilson, A. H., Slate, F. O. Shear capacity of reinforced concrete beams using high-strength concrete. In: ACI Journal Proceedings; 1986; p. 290-296. doi:10.14359/10432.

[20] Wight James, K., Sozen Mete, A. Strength Decay of RC Columns under Shear Reversals. Journal of the Structural Division, 1975; 101: 1053-1065. doi:10.1061/JSDEAG.0004048.

[21] Woodward Kyle, A., Jirsa James, O. Influence of Reinforcement on RC Short Column Lateral Resistance. Journal of Structural Engineering, 1984; 110: 90-104. doi:10.1061/(ASCE)0733-9445(1984)110:1(90).

[22] Ascheim, M., Moehle, J. Shear strength and deformability of RC bridge columns subjected to inelastic cyclic displacements. Berkeley (CA): Earthquake Engineering Research Center, University of California, Berkeley; 1992. Report No.: UCB/EERC-92/04.

[23] Ghee, A. B., Priestley, M. J. N., Paulay, T. Seismic Shear Strength of Circular Reinforced Concrete Columns. ACI Structural Journal, 1989; 86: 45-59. doi:10.14359/2634.

[24] Yuk-Lung Wong, T. P., Priestley, M. J. N. Response of Circular Reinforced Concrete Columns to Multi-Directional Seismic Attack. ACI Structural Journal, 1993; 90: 180-191. doi:10.14359/4124.

[25] Bengar, H. A., Kiadehi, M. A., Shayanfar, J., Nazari, M. Effective flexural rigidities for RC beams and columns with steel fiber. Steel and Composite Structures, An International Journal, 2020; 34: 453-465. doi:10.12989/scs.2020.34.3.453.

[26] Lynn, A. C. Seismic evaluation of existing reinforced concrete building columns (PhD Thesis). Berkeley (CA): University of California, Berkeley; 2001.

[27] Pan, Z., Li, B. Truss-Arch Model for Shear Strength of Shear-Critical Reinforced Concrete Columns. Journal of Structural Engineering, 2013; 139: 548-560. doi:10.1061/(ASCE)ST.1943-541X.0000677.

[28] Duong, K. V., Sheikh, S. A., Vecchio, F. J. Seismic behavior of shear-critical reinforced concrete frame: Experimental investigation. ACI Structural Journal, 2007; 104: 304-313. doi:10.14359/18620.

[29] Lee, J.-Y., Watanabe, F. Shear deterioration of reinforced concrete beams subjected to reversed cyclic loading. ACI Structural Journal, 2003; 100: 480-489. doi:10.14359/12657.

[30] Lee, J. Y., Watanabe, F. Predicting the longitudinal axial strain in the plastic hinge regions of reinforced concrete beams subjected to reversed cyclic loading. Engineering Structures, 2003; 25: 927-939. doi:10.1016/S0141-0296(03)00026-9.

[31] Ho, J. C. M., Pam, H. J. Inelastic design of low-axially loaded high-strength reinforced concrete columns. Engineering Structures, 2003; 25: 1083-1096. doi:10.1016/S0141-0296(03)00050-6.

[32] Moretti, M., Tassios, T. P. Behaviour of short columns subjected to cyclic shear displacements: Experimental results. Engineering Structures, 2007; 29: 2018-2029. doi:10.1016/j.engstruct.2006.11.001.

[33] Pendyala, R. S., Mendis, P. Experimental study on shear strength of high-strength concrete beams. ACI Structural Journal, 2000; 97: 564-571. doi:10.14359/7421.

[34] American Concrete Institute (ACI). ACI 318-08: Building Code Requirements for Structural Concrete and Commentary. Farmington Hills (MI): ACI; 2008. doi:10.14359/51716937.

[35] Federal Emergency Management Agency (FEMA). FEMA Publication 273: NEHRP Guidelines for the seismic rehabilitation of buildings. Washington, D.C. (US): FEMA; 1997.

[36] New Zealand Standard (NZS). NZS 3101.1: Design of concrete structures. Wellington (NZ): NZS; 2006.

[37] Akbarzadeh Bengar, H., Abdollahtabar, M., Shayanfar, J. Predicting the Ductility of RC Beams Using Nonlinear Regression and ANN. Iranian Journal of Science and Technology, Transactions of Civil Engineering, 2016; 40: 297-310. doi:10.1007/s40996-016-0033-0.

[38] Akbarzadeh Bengar, H., Shayanfar, J. Seismic performance of RC frames joints retrofitted by CFRP composites. In: Proceedings of the 2th International and the 6th National Conference on Earthquake & Structures; 2015 Oct 14–15; Kerman, Iran. p. 1-10.

[39] Tariq, M., Khan, A., Ullah, A., Shayanfar, J., Niaz, M. Improved Shear Strength Prediction Model of Steel Fiber Reinforced Concrete Beams by Adopting Gene Expression Programming. Materials, 2022; 15: 3758. doi:10.3390/ma15113758.

[40] Tariq, M., Khan, A., Shayanfar, J., Hanif, M. U., Ullah, A. A regression model for predicting the shear strength of RC knee joint subjected to opening and closing moment. Journal of Building Engineering, 2021; 41: 102727. doi:10.1016/j.jobe.2021.102727.

[41] Akbarzadeh Bengar, H., Shayanfar, J., Seyedpoor, S. M. An artificial neural network (ANN) model for predicting themoment-rotation of exterior RC beam–column jointsstrengthened by CFRP composites. In: Proceedings of the 2th International and the 6th National Conference on Earthquake & Structures; 2015 Oct 14–15; Kerman, Iran. p. 11-20.

[42] Abedi, M., Shayanfar, J., Al-Jabri, K. Infrastructure damage assessment via machine learning approaches: a systematic review. Asian Journal of Civil Engineering, 2023; 24: 3823-3852. doi:10.1007/s42107-023-00748-5.

[43] Park, H.-G., Yu, E.-J., Choi, K.-K. Shear-strength degradation model for RC columns subjected to cyclic loading. Engineering Structures, 2012; 34: 187-197. doi:10.1016/j.engstruct.2011.08.041.

[44] Chen, W. F. Plasticity in Reinforced Concrete. 1st ed. Plantation (FL): J. Ross Publishing; 2007.

[45] Priestley, M. J. N., Verma, R., Xiao, Y. Seismic Shear Strength of Reinforced Concrete Columns. Journal of Structural Engineering, 1994; 120: 2310-2329. doi:10.1061/(ASCE)0733-9445(1994)120:8(2310).

[46] Sezen, H., Moehle Jack, P. Shear Strength Model for Lightly Reinforced Concrete Columns. Journal of Structural Engineering, 2004; 130: 1692-1703. doi:10.1061/(ASCE)0733-9445(2004)130:11(1692).

[47] Ohue, M., Morimoto, H., Fujii, S., Morita, S. Behavior of R.C. Short Columns Failing in Splitting Bond-shear Under Dynamic Lateral Loading. ed. Tokyo (JP): Japan Concrete Institute; 1985.

[48] Esaki, F. Reinforcing effect of steel plate hoops on ductility of R/C square columns. In: 11th World Conference on Earthquake Engineering; 1996; Acapulco (MX). p. 196.

[49] Li, X. Reinforced concrete columns under seismic lateral force and varying axial load (PhD Thesis). Christchurch (NZ): University of Canterbury; 1994.

[50] Saatcioglu, M., Ozcebe, G. Response of reinforced concrete columns to simulated seismic loading. ACI Structural Journal, 1989; 86: 3-12. doi:10.14359/2607.

[51] Yalcin, C. Seismic evaluation and retrofit of existing reinforced concrete bridge columns (PhD Thesis). Ottawa (CA): University of Ottawa; 1998.

[52] Hirosawa, M. A list of past experimental results of reinforced concrete columns. 1st ed. Tokyo (JP): Building Research Institute Ministry of Construction; 1973.

[53] Xiao, Y., Martirossyan, A. Seismic Performance of High-Strength Concrete Columns. Journal of Structural Engineering, 1998; 124: 241-251. doi:10.1061/(ASCE)0733-9445(1998)124:3(241).

[54] Yoshimura, M. Formulation of post-peak behavior of old reinforced concrete columns until collapse. In: The 14th World Conference Earthquake Engineering; 2008 Oct 12–17; Beijing, China. p. 15-26.

[55] Yoshimura, M., Takaine, Y., Nakamura, T. Collapse drift of reinforced concrete columns. Journal of Structural and Construction Engineering (Transactions of AIJ), 2003; 68: 153-160. doi:10.3130/aijs.68.153_5.

[56] Nakamura, T., Yoshimura, M. Simulation of old reinforced concrete column collapse by pseudo-dynamic test method. In: 15th World conference on earthquake engineering; 2012 Sep 24-28; Lisbon, Portugal. p. 0-20.

[57] Nakamura, T., Yoshimura, M. Gravity load collapse of reinforced concrete columns with decreased axial load. In: Proceedings of the 2nd European Conference on Earthquake Engineering and Seismology, Istanbul, Turkey; 2014 Aug 24-25; Istanbul, Turkey. p. 25-29.

[58] Li, Y.-A., Huang, Y.-T., Hwang, S.-J. Seismic response of reinforced concrete short columns failed in shear. ACI Structural Journal, 2014; 111: 945-954. doi:10.14359/51686780.

[59] Ramirez, H., Jirsa, J. O. Effect of axial load on shear behavior of short RC columns under cyclic lateral deformations. Austin (TX): University of Texas at Austin. Phil M. Ferguson Structural Engineering Laboratory; 1980. Report No.: ENV77-20816.

[60] Bett, B., Jirsa, J., Klingner, R. Behavior of strengthened and repaired reinforced concrete columns under cyclic deformations. Austin (TX): University of Texas at Austin. Phil M. Ferguson Structural Engineering Laboratory; 1985. Report No.: 85-3.

[61] Umehara, H. Shear strength and deterioration of short reinforced concrete columns under cyclic deformations (PhD Thesis). Austin (TX): University of Texas at Austin; 1983.

[62] Ousalem, H., Kabeyasawa, T., Tasai, A. Evaluation of ultimate deformation capacity at axial load collapse of reinforced concrete columns. In: Proceedings of 13th world conference on earthquake engineering; 2004 Aug 1-4; Vancouver, B. C., Canada. p. 370.

[63] Aboutaha, R. S., Engelhardt, M. D., Jirsa, J. O., Kreger, M. E. Rehabilitation of shear critical concrete columns by use of rectangular steel jackets. ACI Structural Journal, 1999; 96: 68-78. doi:10.14359/597.

[64] Woods, C. Displacement demand effects in vulnerable reinforced concrete columns (PhD Thesis). Lawrence (KS): University of Kansas; 2010.

[65] Boys, A., Bull, D., Pampanin, S. Seismic performance assessment of inadequately detailed reinforced concrete columns. In: 2008 New Zealand Society for Earthquake Engineering (NZSEE) Conference; 2008 Apr 11-13; Wellington, New Zealand. p. 29.

[66] Kogoma, I., Hayashida, T., Minowa, C. Experimental studies on the collapse of RC columns during strong earthquake motions. In: 10th World Conference on Earthquake Engineering; 1992 Jul 19–24; Madrid, Spain. p. 3013-3017.

[67] Choi, K.-K., Truong, G. T., Kim, J.-C. Seismic performance of lightly shear reinforced RC columns. Engineering Structures, 2016; 126: 490-504. doi:10.1016/j.engstruct.2016.07.060.

[68] Ghannoum Wassim, M., Moehle Jack, P. Rotation-Based Shear Failure Model for Lightly Confined RC Columns. Journal of Structural Engineering, 2012; 138: 1267-1278. doi:10.1061/(ASCE)ST.1943-541X.0000555.

[69] Elwood, K. J., Moehle, J. P. Dynamic collapse analysis for a reinforced concrete frame sustaining shear and axial failures. Earthquake Engineering & Structural Dynamics, 2008; 37: 991-1012. doi:10.1002/eqe.787.

[70] Howser, R., Laskar, A., Mo, Y. Seismic interaction of flexural ductility and shear capacity in reinforced concrete columns. Structural engineering and mechanics: An international journal, 2010; 35: 593-616. doi:10.12989/sem.2010.35.5.593.

[71] Shin, M., Choi, Y. Y., Sun, C.-H., Kim, I.-H. Shear strength model for reinforced concrete rectangular hollow columns. Engineering Structures, 2013; 56: 958-969. doi:10.1016/j.engstruct.2013.06.015.

[72] Kowalsky, M. J., Priestley, M. N. Improved analytical model for shear strength of circular reinforced concrete columns in seismic regions. ACI Structural Journal, 2000; 97: 388-396. doi:10.14359/4633.

[73] State of California Department of Transportation. Caltrans Version 2.0: Caltrans Seismic Design Criteria. Sacramento (CA): Caltrans; 2019.